Anal. Bioanal. Electrochem., Vol. 18, No. 1, 2026, 96-131
https://www.doi.org/10.22034/abec.2026.741082

Analytical & Bioanalytical Electrochemistry

Review

V_2O_5-Based Cathodes in Aqueous Zn-Ion Batteries: From Structural Modifications to Superior Performance

Sepideh Nasimi,[1] Mehran Javanbakht,[1] and Khadijeh Hooshyari[2]

[1]*Department of Chemistry, Amirkabir University of Technology, Tehran, Iran*
[2]*Department of Chemistry, Iran University of Science and Technology, Tehran 16846-1314, Iran*

*Corresponding Author, Tel.: +98-2164545806
E-Mail: mehranjavanbakht@gmail.com

Received: 3 January 2026 / Received in revised form: 13 February 2026 / Accepted: 20 February 2026 / Published online: 28 February 2026

Abstract- Zinc-ion batteries have been proposed as promising alternatives for energy storage systems owing to their high safety, low cost, and environmental compatibility. Among them, V_2O_5 is considered one of the most important candidates for use as a cathode in these batteries because of its high specific capacity, multiple oxidation states, and suitable layered structure. However, challenges such as low conductivity, dissolution of vanadium in aqueous electrolytes, structural changes during the charge and discharge processes, and formation of unstable by-products have limited the performance of this material. Recently, various strategies have been introduced to overcome these problems, including interlayer insertion of cations and water molecules, metal doping, surface modification with conductive coatings, and electrolyte optimization. These modifications have led to expanded interlayer spacing, improved structural stability, enhanced ionic and electronic conductivity, and ultimately increased specific capacity and cycle life in V_2O_5-based batteries. A review of recent research suggests that structural and compositional engineering of V_2O_5 could pave the way for the development of stable and high-performance cathodes and significantly support their technological development in future energy storage applications.

Keywords- Aqueous zinc-ion batteries; Cathodes; Vanadium Pentoxide; Electrochemical mechanism; Modifications; Interlayer engineering

1. INTRODUCTION

With the increasing global demand for energy, the world has gradually become a more interconnected system, while the natural capacity of the Earth remains limited. Energy and related services play a fundamental role in promoting social welfare, economic development,

health, and quality of life worldwide. In all societies, energy supply is essential to meet basic needs, such as sanitation, lighting, cooking, ventilation, transportation, and communication. In addition, energy is the driving force behind production and economic processes. However, there are two major challenges to achieving a sustainable energy future: (1) securing a sustainable energy supply and (2) reducing the environmental impacts of its consumption. In this context, inequality in energy access, especially in rural areas, has become a serious global concern. Statistics show that approximately 1.4 billion people still do not have access to electricity, and 85% of them live in rural areas [1].

This trend highlights the need to develop sustainable and inclusive approaches that ensure equitable access to energy, particularly in underserved regions. The large-scale transformation of energy systems and the continuous shift toward increased utilization of renewable resources have rendered the development of advanced energy storage technologies a strategic priority. Although renewable energy sources such as solar, wind, and tidal power are considered promising alternatives for reducing reliance on fossil fuels, their inherent intermittency necessitates the deployment of efficient energy storage systems to maintain grid stability and ensure reliable operation. Among the available options, batteries are the most widely implemented electrochemical energy storage technology for on-demand energy storage and release.

Batteries are generally classified into two main categories. Primary (non-rechargeable) batteries, including zinc–carbon, alkaline manganese, and lithium–manganese dioxide systems, are designed for single-use applications and, despite their relatively high energy density, are unsuitable for large-scale energy storage due to the irreversibility of their electrochemical reactions. In contrast, secondary (rechargeable) batteries, such as lead–acid, nickel–cadmium, nickel–metal hydride, and particularly lithium-ion batteries, are capable of repeated charge–discharge cycles and have emerged as the dominant technology across a wide range of applications, from portable electronic devices to electric vehicles and stationary energy storage systems, owing to their high energy density, favorable cycle life, and desirable power performance [2].

Despite their impressive advantages, lithium-ion batteries face serious challenges, including the scarcity of lithium resources, high cost of extraction, and safety hazards posed by toxic and flammable organic electrolytes, which have limited their widespread use. Consequently, research has focused on alternatives with lower costs, higher safety, and abundant resources.

One promising path is the development of multivalent ion batteries, such as manganese, zinc, and aluminum ion batteries, which offer greater energy storage capacity owing to the transfer of multiple electrons per ion and greater volumetric density. Among these options, ZIBs hold a unique position**.** Zinc, as an abundant, cheap, and safe metal, provides a high specific capacity of 820 mAh/g and an impressive volumetric density of 5851 mAh/cm^3, which

is much higher than similar systems such as magnesium (3832 mAh/cm³) and calcium (2073 mAh/cm³).

In addition, the favorable electrode potential of -0.76 V vs. the standard hydrogen electrode and the use of aqueous electrolytes with ionic conductivity greater than 1 S/cm^3 have reduced the safety concerns associated with organic electrolytes in lithium-ion batteries. These features have made ZIBs an attractive option for grid-scale energy storage as well as emerging applications such as flexible electronics [3].

However, the main obstacle to improving the performance of ZIBs is the development of effective cathode materials for them. Cathode materials play a critical role in determining the ion storage capacity, reaction kinetics, and overall cycling stability. Various classes of cathode materials have been investigated, including vanadium-based compounds, manganese, Prussian blue analogs, and organic compounds. Among these groups, vanadium compounds have received particular attention.

Vanadium, with its diverse oxidation states ranging from +3 to +5, has a high capacity of 589 mAh/g and provides a suitable substrate for storing and rapidly transporting Zn^{2+} owing to its diverse structures. However, challenges such as vanadium dissolution in the electrolyte, phase changes during charge/discharge cycles, and the formation of unstable byproducts such as $Zn_3(OH)_2V_2O_7{\cdot}2H_2O$ hinder the long-term stability of these cathodes. Therefore, recent research has focused on in-depth investigations of the energy storage mechanism, structural evolution of vanadium cathodes during cycling, and strategies for performance development. A review of these studies can provide new insights into the fundamental challenges in this field and pave the way for the development of ZIBs with higher efficiencies and improved stabilities [4].

The main objective of this review is to discuss the status of V_2O_5 as one of the most widely used and promising cathode materials in zinc-ion batteries. Since the introduction of these systems in 2016, extensive research has been conducted to improve their performance, increase their capacity, and extend their lifespan. This review provides a comprehensive overview of recent scientific progress in this field based on a critical evaluation of recent results [5].

2. CATHODE MATERIALS FOR ZINC-ION BATTERIES

The cathode is a critical component of battery systems. In recent years, significant research efforts in the field of ZIBs have focused on developing high-performance cathode materials. The primary objective is to identify materials that can possess stable structures with high ion-storage capacities. Beyond stability during the charge and discharge cycles, these materials must maintain a high-capacity retention over extended periods. Various compounds have been proposed as suitable cathode materials for ZIBs, including manganese oxide-based compounds, vanadium oxide-based compounds, Prussian blue analogs, and organic materials. These candidates have been identified as primary choices owing to their distinct properties, including

capacity, structural stability, and electrochemical kinetics. Parameters such as operating potential, specific capacity, cyclic stability, and environmental impact critically influence the performance of batteries. These cathode materials are discussed in detail in the following sections to accurately analyze and compare their performances under various conditions. Future studies in this area aim to optimize these materials to improve the efficiency and lifespan of ZIBs, thereby facilitating their widespread application in renewable energy and energy storage technologies [6].

2.1. Manganese oxide–based cathode materials for zinc-ion batteries

Manganese oxide-based cathodes have attracted considerable attention in the development of ZIBs because of their numerous advantages. Manganese is the tenth most abundant element in the Earth's crust, and exhibits variable oxidation states (+2, +3, +4, and +7). It is biocompatible, and the crystal structures of its oxides possess a superior capacity for the intercalation and reversible release of Zn^{2+} [7]. Furthermore, polyvalent manganese oxides exhibit diverse crystal structures, among which MnO_2 displays the greatest structural diversity [8]. Manganese dioxide is known as the main crystal skeleton with an octahedral unit composed of six oxygen atoms and one manganese atom. Various MnO_2 polymorphs have been widely used as cathodes in ZIBs .These cathodes have a capacity exceeding 300 mAh/g. However, ion dissolution leads to a decrease in the cyclic stability [7]. Due to the high theoretical capacity and voltage of about 0.8–1.8, non-toxicity, and natural abundance, manganese oxides are the most widely used cathode materials in ZIBs. To date, MnO_2, Mn_2O_3, and Mn_3O_4 have been reported as suitable materials. Various polymorphs of MnO_2 include α-MnO_2, β-MnO_2, γ-MnO_2, ε-MnO_2, and δ-MnO_2 [9]. Despite significant improvements, manganese-based batteries often suffer from rapid capacity loss during cycling and poor performance at high rates [10]. In a previous study, α-MnO_2 was introduced as a cathode material for aqueous zinc-ion batteries. The α-MnO_2 cathode delivered a specific capacity of 210 mAh/g at a current density of 200 mA/g, and no noticeable capacity fading was observed after 50 cycles at a high current density of 1 A/g, indicating excellent cycling stability [11]. For example, in recent research, the doping method was used to improve and modify the performance of manganese oxide-based cathode materials.

In this study, we focused on improving the performance of manganese oxide-based cathode materials in ZIBs, which typically face challenges due to low conductivity and capacity loss during charge and discharge cycles. To overcome these limitations, pulsed potential electrodeposition has been successfully employed to synthesize a nickel-doped $ZnMn_2O_4/Mn_2O_3$ biphasic nanocomposite. Ni doping was performed to improve the electrical conductivity, increase the structural stability, and optimize the electrochemical behavior of the cathode. Studies showed that the presence of Ni^{2+} ions reduced the crystallite size, increased the specific surface area to approximately 145 m^2/g, and resulted in a more uniform distribution

of elements in the nanocomposite structure Among all samples, the Ni/Mn-modified cathode with a Ni: Mn molar ratio of 0.07:1 exhibited superior electrochemical performance, delivering a high specific capacity of 235.1 mAh/g at 0.2 A/g, which is markedly higher than that of the undoped material (215 mAh/g). Notably, upon prolonged cycling at a high current density of 2 A/g, the optimized sample maintained a reversible capacity of 114.67 mAh/g after 3000 cycles, corresponding to an outstanding capacity retention of 91.32%, in sharp contrast to the undoped electrode, which retained only 64.54% of its initial capacity [12].

2.2. Cathode materials based on Prussian blue analogues in zinc-ion batteries

Although these materials exhibit a relatively high operating voltage in the range of 1.5–1.8 V, their theoretical capacities remain below 100 mAh/g, which severely limits their achievable energy density. Moreover, inherent issues, including poor long-term cycling stability and low intrinsic electronic conductivity, hinder their application in high-performance aqueous zinc-ion batteries. The crystal structures of these compounds are generally represented by the formula $A_xM_1[M_2(CN)_6]_y \cdot nH_2O$, where A refers to alkali metal ions and M denotes transition metals. The presence of an open and porous framework facilitates reversible Zn^{2+} intercalation/deintercalation within the host lattice. Such structural features, including abundant pores and lattice water molecules, are formed as a consequence of rapid deposition. These attributes significantly influence the electrochemical performance, particularly by improving the structural integrity and long-term cycling stability of aqueous ZIBs [10]. In 2014, the first aqueous ZIBs utilizing a zinc hexacyanoferrate-based Prussian blue analog cathode were demonstrated, delivering a relatively high operating voltage of ~1.7 V. Subsequently, PBA-type cathode materials incorporating transition metals such as Cu, Mn, and Fe have attracted considerable research interest. Despite their favorable voltage characteristics and structural stability, the inherently low specific capacity of PBAs remains a critical challenge that restricts their practical application in high-energy-density systems [7].

2.3. Vanadium oxide–based cathode materials for zinc-ion batteries

Vanadium, ranked as the 20th most abundant element in the Earth's crust, has attracted considerable attention as a promising electrode material for metal-ion energy storage systems, especially aqueous zinc-ion batteries, owing to its multivalent redox chemistry (V^{2+}–V^{5+}) and high redox activity. Vanadium oxides are composed of V–O polyhedral building blocks with flexible coordination geometries, including tetrahedral, square-pyramidal, trigonal-bipyramidal, and distorted octahedral motifs. This intrinsic structural versatility, together with the tunable oxidation states of vanadium, facilitates rapid and reversible Zn^{2+} storage. Furthermore, interlayer cations play a crucial role in stabilizing layered and chain-structured vanadium oxides, thereby enhancing their structural robustness and enabling highly reversible Zn^{2+} intercalation/deintercalation [10]. The first practical demonstration of vanadium oxide as

a cathode material for aqueous ZIBs was reported in 2016, when Kondo et al. developed a layered $Zn_{0.25}V_2O_5 \cdot nH_2O$ cathode, which delivered a high reversible capacity of approximately 300 mAh/g and maintained approximately 80% of its initial capacity after 1000 charge–discharge cycles. Since then, extensive research efforts have been devoted to vanadium-based cathode materials, which have garnered increasing attention owing to their high specific capacity and superior electrochemical performance compared with manganese oxides and Prussian blue analogs. Nevertheless, the intrinsically low operating voltage of around 0.8 V versus Zn/Zn^{2+} remains a critical bottleneck for their practical application [7].

Table 1 comprehensively reports the main characteristics, advantages, and disadvantages of various cathode materials for ZIBs.

Table 1. Overview of types of cathode materials for ZIBs and key performance indicators

Cathode materials	**Capacity (mAh/g)**	**Disadvantages**	**Advantages**	**Average Voltage (V)**
Vanadium based	>300	• Poor electrical conductivity • Low average voltage	• Multi-electron redox reactions • High reversible capacity	0.8-1
Manganese oxide-based	~308	• Dissolution of manganese ions • Phase change • Poor electrical conductivity • Low specific capacity	• Diverse structure • Rich valence states	1.35
Prussian blue analogue-based	<100	• High voltage • Poor cyclic stability • Low Coulombic efficiency	• Open structure • Sufficient redox active sites • Stable crystal structure	1.5-1.8
Organic compound-based	Very little	• Poor electrical conductivity • Easy dissolution in electrolyte • Complex structure	• Simple synthesis process • Flexible	0.7-1.7

Overall, vanadium-based cathode materials offer significant advantages over alternative cathodes because of their multivalent redox behavior and high reversible Zn^{2+} storage capability. However, inherent issues such as low intrinsic electronic conductivity and relatively low average operating voltage continue to impede their large-scale application in aqueous ZIBs [13].

Figure 1 illustrates the publication trend of research articles related to vanadium-based ZIBs and vanadium oxide compounds from 2019 to 2023. Overall, the number of studies focusing on vanadium pentoxide–based ZIBs has increased markedly compared to other

vanadium-based compounds during this period. This pronounced growth can be primarily attributed to the outstanding electrochemical advantages and broad application potential of V_2O_5 cathode for ZIBs.

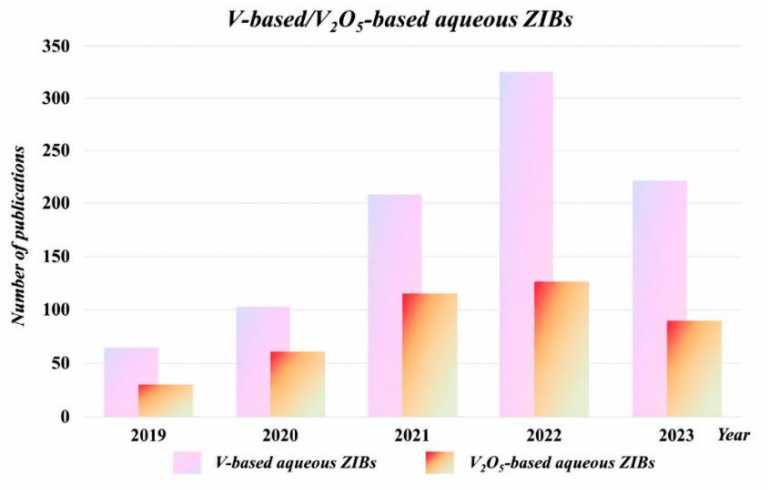

Figure 1. Statistical comparison of published papers on vanadium-based cathodes in ZIBs over the past three years [14]

V_2O_5 has emerged as a prominent cathode material for aqueous ZIBs because of its high specific capacity, robust cycling stability, and reversible Zn^{2+} storage behavior.

In addition, its intrinsic compatibility with aqueous electrolytes and favorable thermal stability endow V_2O_5-based systems with enhanced safety characteristics and improved overall electrochemical efficiency [2].

V_2O_5 exhibits a typical layered structure constructed from stacked square-pyramidal VO_5 units connected via edge or corner-sharing. Within this framework, strong covalent bonding dominates the intralayer network, whereas weak van der Waals interactions and hydrogen bonding govern the interlayer region. This layered architecture facilitates fast Zn^{2+} diffusion between adjacent layers, thereby enabling excellent rate capability. In 2018, Zhang et al. reported a Zn–V_2O_5 based cathode for aqueous zinc-ion batteries, which demonstrated a high energy density along with favorable cycling stability. In addition to its outstanding electrochemical performance, this cathode material also maintains stable operation over a wide temperature range [15].

3. ENERGY STORAGE MECHANISM IN V_2O_5-BASED ZINC-ION BATTERIES

A comprehensive understanding of energy storage mechanisms is essential for the rational design and development of advanced electrode materials for battery systems. In the currently reported aqueous ZIBs employing layered V_2O_5-based cathodes, the Zn^{2+} storage behavior can generally be classified into four dominant mechanisms:

3.1. Insertion and extraction of Zn^{2+}

In aqueous ZIBs systems, the energy storage mechanism resembles that of lithium-ion batteries, involving the reversible shuttling of Zn^{2+} ions between the cathode and anode. During the discharge process, metallic Zn at the anode undergoes oxidation to generate Zn^{2+} ions, which subsequently migrate through the electrolyte and are inserted into the V_2O_5 cathode. Concurrently, the vanadium ions are reduced from higher oxidation states (V^{5+}) to lower valence states such as V^{4+} or V^{3+}. Meanwhile, electrons flow from the anode to the cathode through an external circuit, enabling the conversion of chemical energy into electrical energy. During the charging process, Zn^{2+} ions are extracted from the cathode and transported back to the anode, where they are reduced and redeposited as metallic Zn. To maintain charge neutrality, electrons migrate from the cathode to the anode via an external circuit, thereby converting electrical energy back into chemical energy. This reversible Zn^{2+} insertion/extraction process is typically accompanied by variations in the interlayer spacing of the cathode material [13].

The electrochemical performance of rechargeable batteries operating via Zn^{2+} insertion/extraction is fundamentally governed by the interaction between the host electrode framework and the incoming charge carriers. Among various factors, the ionic charge of the inserted species plays a decisive role in determining the electrochemical behavior of the batteries. Recent studies have demonstrated that aqueous battery systems based on multivalent ion insertion exhibit significantly superior performance to their non-aqueous counterparts. This enhancement arises from the co-insertion of water molecules alongside Zn^{2+} ions, which effectively act as a buffering medium to screen the strong electrostatic interactions associated with the multivalent ions. Consequently, the charge density of Zn^{2+} ions are moderated, leading to reduced interfacial charge-transfer energy barriers at the electrode–electrolyte interface. Furthermore, the structural flexibility of the host electrode materials facilitates facile Zn^{2+} insertion and extraction, thereby enabling fast reaction kinetics and superior rate capabilities over a wide range of current densities. Moreover, the ability of the electrode to accommodate mechanical stresses induced during repeated charge–discharge cycling, together with effective interparticle contact, continuous conductive networks provided by carbonaceous additives, and a compact yet mechanically flexible electrode architecture, collectively contribute to enhanced structural stability and significantly improved electrochemical performance of rechargeable battery systems [14].

3.2. Insertion and extraction of Zn^{2+} and H^+

In 2018, Wan et al. proposed a dual-ion energy storage mechanism involving the simultaneous insertion of two ionic species into the crystal structure of a sodium vanadate cathode [16]. One of the key energy storage mechanisms in vanadium-based cathodes is the co-insertion and extraction of H^+ and Zn^{2+} ions. This mechanism has been widely reported in

various vanadium-containing compounds, including $VO_2 \cdot 0.45H_2O$, $V_{10}O_{24} \cdot 1.2H_2O$, VO_x, $Mn_{0.31}V_3O_7 \cdot 1.4H_2O$, $MgV_2O_6 \cdot 1.7H_2O$, and related materials. A common characteristic of these compounds is their layered crystal frameworks, which provide favorable pathways for the simultaneous accommodation of dual ionic species. Thermodynamic and kinetic analyses suggest that H^+ insertion occurs preferentially prior to Zn^{2+} insertion, owing to the smaller ionic radius and lower insertion energy of protons compared with Zn^{2+} ions. In general, this energy storage process proceeds via two sequential steps: initial H^+ insertion in the high-voltage region, followed by Zn^{2+} insertion at lower operating voltages in their interlayer space [14].

The insertion of H^+ effectively regulates the charge distribution within the interlayer galleries and simultaneously expands the interlayer spacing, thereby reducing the diffusion energy barrier for Zn^{2+} migration between adjacent layers. Consequently, this proton-assisted structural modulation facilitates faster Zn^{2+} transport kinetics and significantly enhances the ionic migration rate [3]. The ion storage mechanism in hydrated VO_2 cathodes was investigated by Zhou. Extensive evidence that hydrogen and Zn^{2+} play a simultaneous and cooperative role in ion storage in hydrated VO_2. Density functional theory calculations show that in this mechanism, hydrogen ion entry occurs mainly in the early stages of discharge, whereas Zn^{2+} entry is observed more in the late stages of discharge [17].

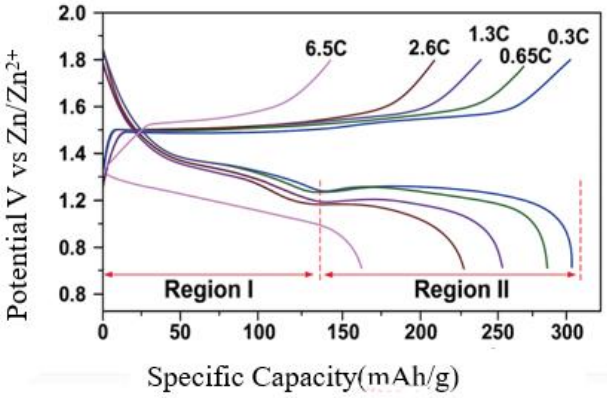

Figure 2. Galvanostatic charge and discharge curves at different C-rates; reprinted with permission from [18]

During the early stage of discharge, H^+ insertion into the host lattice reduces the local H^+ concentration near the electrode surface. At this stage, the concentration of OH^- in the electrolyte remained relatively low, thereby effectively suppressing the formation of undesirable by-products such as zinc hydroxide sulfate. As the discharge proceeds and Zn^{2+} intercalation becomes dominant, further proton consumption results in an increased OH^- concentration at the electrode–electrolyte interface, which facilitates the nucleation and growth of $Zn(OH)_2$ deposits on the electrode surface. Moreover, simultaneous co-insertion of Zn^{2+} and H^+ ions can occur, ultimately leading to the generation of parasitic side products within the

electrolyte [14]. Wang et al. [18] reported an intriguing stepwise ion-storage mechanism, in which the sequential intercalation and deintercalation of Zn^{2+} and H^+ were accompanied by distinct electrochemical signatures. The charge–discharge curves could be clearly divided into two separate potential regions, and variations in the continuous charge–discharge rates resulted in different behaviors across these regions. Galvanostatic intermittent titration technique (GITT) analysis revealed that Region I was dominated by H^+ insertion/extraction, exhibiting a relatively smaller potential drop compared to Region II. In contrast, Region II, associated with Zn^{2+} intercalation, displayed a significantly higher overpotential, approximately 0.08 V greater, reaching approximately 0.6 V above that observed in Region I.

3.3. Substitution and insertion mechanism

Shan et al. proposed a hybrid substitution–intercalation energy-storage mechanism for aqueous zinc-ion batteries. This mechanism can be divided into two primary steps:

(i) Ag^+ substitution: In the initial stage of discharge, incoming Zn^{2+} ions replace Ag^+ ions within the $Ag_{0.4}V_2O_5$ host lattice. This ion-exchange process induced a phase transformation, leading to the formation of the $Zn_2(V_3O_8)_2$ phase.

(ii) Zn^{2+} intercalation: Following the substitution reaction, Zn^{2+} ions can further intercalate into the layered frameworks of the host materials, including $Ag_{0.4}V_2O_5$ and the newly formed $Zn_2(V_3O_8)_2$ phase, resulting in various intermediate phases during the discharge process. During the subsequent charging step, Zn^{2+} ions are extracted from the host lattice, and the pristine $Ag_{0.4}V_2O_5$ phase is largely recovered. Notably, a small fraction of Ag^+ ions remain embedded within the structure, forming an internal conductive network within the electrode, which effectively enhances electronic conductivity and thereby improves the overall electrochemical performance of the battery [13].

4. SYNTHESIS STRATEGIES FOR V_2O_5-BASED CATHODE MATERIALS

Various synthesis techniques have been developed for the fabrication of cathode materials, each exhibiting specific merits and inherent limitations. Among these approaches, the hydrothermal method has been extensively employed for preparing V_2O_5-based cathodes. In this process, chemical reactions are conducted in a sealed autoclave under elevated temperature and pressure, with water serving as the reaction medium. The resulting powder is typically formed via a dissolution–recrystallization mechanism, which promotes controlled crystal growth, reduces particle size, and enhances structural homogeneity. Nevertheless, the hydrothermal approach generally requires harsh operating conditions and specialized equipment, rendering it relatively expensive and technically demanding for large-scale production. A closely related synthesis route is the solvothermal method, which is derived from the conventional hydrothermal process. In this approach, precursor solutions undergo reactions in a closed environment, such as an autoclave, typically employing non-aqueous or organic

solvents as reaction media. The solvothermal method effectively suppresses undesired oxidation reactions while facilitating controlled crystal growth and the phase evolution. However, several challenges persist, including relatively low product yield, chemical instability of certain precursor species, and limited scalability for large-scale or industrial production.

Another widely adopted strategy for synthesizing nanostructured cathode materials is the sol–gel method. In this process, precursor compounds are dissolved in an appropriate solvent and undergo hydrolysis to generate highly reactive molecular species. These species subsequently polymerize to form a three-dimensional sol network that gradually evolves into a structurally defined gel. Upon controlled drying and subsequent calcination, nanosized oxide particles and the desired crystalline cathode material were obtained. The sol–gel technique is relatively straightforward and offers excellent chemical homogeneity and high product purity. Nevertheless, inherent limitations such as weak interparticle connectivity, substantial volumetric shrinkage during drying, and particle agglomeration may adversely affect the electrochemical performance of the resulting materials.

In addition, thermal decomposition represents another synthesis route, wherein precursor compounds are decomposed under elevated temperature and pressure to yield thermodynamically stable products. Although this approach is generally more energy-intensive and costly, the resulting materials often exhibit outstanding phase purity and structural robustness, making thermal decomposition particularly attractive for specialized high-performance battery applications [14].

5. CHALLENGES OF V_2O_5 CATHODE MATERIALS IN ZINC-ION BATTERIES

Despite its high theoretical capacity and considerable promise for electrochemical energy storage, V_2O_5 suffers from several intrinsic limitations that severely impede its practical application as a cathode material in aqueous zinc-ion batteries. The most critical challenges include low intrinsic electronic conductivity, strong electrostatic interactions between Zn^{2+} ions and the host lattice, and insufficient structural stability during repeated Zn^{2+} insertion/extraction processes. These issues commonly result in a shortened cycling life, the formation of parasitic by-products, and progressive capacity decay upon prolonged cycling. Furthermore, sluggish ion diffusion kinetics and limited electron transport within the V_2O_5 framework significantly constrain its rate performance, particularly at high current densities where fast charge transfer and reversible redox reactions are essential. Under these conditions, maintaining continuous diffusion pathways and stable redox activity becomes increasingly challenging, leading to pronounced polarization and performance degradation during long-term operation. To address these limitations, extensive efforts have been devoted to structural and compositional engineering strategies, including metal-ion doping, interlayer engineering, hybridization with conductive matrices, and morphological modulation to optimize ion diffusion channels and

enhance mechanical robustness. These approaches have proven effective in alleviating structural collapse, stabilizing the layered architecture of V_2O_5, and improving the Zn^{2+} storage reversibility. Consequently, overcoming these intrinsic challenges is of paramount importance for the development of high-performance, durable V_2O_5-based cathodes for next-generation aqueous Zn-ion energy storage systems.

5.1. Poor electrical conductivity

V_2O_5 features a layered crystal structure with relatively large interlayer spacing, while vanadium predominantly exists in its highest oxidation state (V^{5+}), enabling access to multiple redox couples during electrochemical reactions. In aqueous zinc-ion batteries, Zn^{2+} ions act as multivalent charge carriers, involving multi-electron redox reactions. Consequently, vanadium pentoxide–based cathodes are expected to deliver high specific capacities.

However, the practical electronic conductivity of V_2O_5 remains inherently low because of the limited density of free charge carriers. In vanadium compounds such as V_2O_5, only a small fraction of electrons can be delocalized from the strong V–O covalent bonds, resulting in a low concentration of mobile electrons and holes. This electronic structure significantly restricts electron transport within the cathode framework, thereby limiting the overall electrochemical performance [5].

Low intrinsic electronic conductivity is one of the primary limitations of vanadium oxygen-based materials, which severely constrains their electrochemical performance in rechargeable battery systems. To address this issue, extensive research efforts have been devoted to enhancing the electrical conductivity of vanadium-based cathodes and thereby improving their electrochemical behavior. Representative strategies include hybridization with conductive carbonaceous materials (such as carbon black, graphene, and carbon nanotubes), surface modification via conductive coatings, and integration with conductive polymers to establish efficient electron transport networks [19].

However, recent research efforts have increasingly shifted toward the development of cathode materials with intrinsically high electronic conductivity. Materials such as conductive polymers, selected transition-metal oxides, and structurally engineered organic compounds can deliver favorable electrochemical performance without relying on external conductive additives. This intrinsic conductivity not only enhances energy storage efficiency but also simplifies electrode fabrication processes and reduces overall manufacturing costs.

Moreover, recent advances have demonstrated that the incorporation of conductive metal–organic frameworks (MOFs) or their derivatives, as well as the integration of carbon nanotubes with cathode materials, plays a pivotal role in improving electronic conductivity and long-term cycling stability. Overall, the synergistic combination of materials engineering strategies and innovative synthesis approaches offers a promising pathway for overcoming the conductivity limitations of cathode materials in aqueous ZIBs [19].

5.2. Damage induced by electrostatic interactions

Owing to the high charge density of Zn^{2+} ions, their diffusion kinetics within the host lattice are inherently sluggish, leading to the gradual accumulation of Zn^{2+} species within the framework. Once the local Zn^{2+} concentration exceeds a critical threshold, irreversible phase transformations may occur. Strong Coulombic interactions between Zn^{2+} ions and anionic species in the cathode lattice result in ion trapping and disruption of local charge neutrality, thereby inducing lattice distortion and the formation of parasitic by-products.

Furthermore, these pronounced electrostatic interactions facilitate the strong coordination of Zn^{2+} ions with the interlayer oxygen atoms in the modified V_2O_5 frameworks. Consequently, pre-intercalated or interlayer-stabilizing ions may be expelled from the lattice into the electrolyte, ultimately causing rapid capacity decay during prolonged cycling. Therefore, alleviating the detrimental effects of electrostatic stress is of critical importance and can be partially achieved through defect engineering strategies or by introducing guest ions or molecules into the host lattice to modulate the charge distribution and weaken Coulombic interactions [5].

5.3. Vanadium dissolution

Vanadium dissolution is one of the most critical degradation mechanisms affecting the electrochemical performance of vanadium-based cathodes. This phenomenon not only results in the continuous loss of electrochemically active material from the cathode but also leads to the migration and subsequent deposition of dissolved vanadium species onto the anode surface, forming a resistive passivation layer. Such a parasitic interfacial layer severely impairs charge-transfer kinetics, disrupts electrode reversibility, and ultimately shortens the long-term cycling life of the battery system. The extent of vanadium dissolution was strongly correlated with cycling duration and progressively intensified with prolonged cycling. Moreover, operating at low current densities typically exacerbates vanadium dissolution, resulting in pronounced capacity fading. In contrast, cycling at high current densities tends to suppress vanadium dissolution owing to the shortened reaction times, thereby enabling more stable long-term electrochemical performance. Overall, vanadium dissolution is widely recognized as a primary contributor to the poor cycling stability of many vanadium-based cathode materials. The redox behavior of cathode materials is strongly influenced by both the nature of the salt species and the pH of the aqueous electrolyte. Compared with alkaline electrolytes, mildly acidic aqueous electrolytes are generally regarded as more favorable owing to their reduced corrosivity and improved interfacial compatibility with zinc metal anodes. However, such mildly acidic environments can compromise the chemical and electrochemical stability of the cathode material, promoting the dissolution of electrochemically active species in the electrolyte. This degradation process is further aggravated by the increased proton concentration arising from water dissociation, which accelerates parasitic reactions and structural degradation. As a

consequence, progressive dissolution and structural destabilization may ultimately lead to partial collapse of the cathode framework, thereby severely limiting the long-term cycling stability and service life of the battery [10]. The dissolution of cathode materials can be effectively suppressed through electrolyte regulation by introducing specific salt additives. Chen et al. demonstrated that the incorporation of Na_2SO_4 into a $ZnSO_4$-based electrolyte can modify the dissolution equilibrium of sodium species in a $NaV_3O_8 \cdot 1.5H_2O$ cathode, thereby inhibiting further dissolution of the active material. By immersing $NaV_3O_8 \cdot 1.5H_2O$ electrodes in $ZnSO_4$ electrolytes containing different concentrations of Na_2SO_4, they found that when the Na_2SO_4 concentration reached 1 M, the electrolyte remained clear and colorless even after 24 h of static soaking, indicating a substantially suppressed cathode dissolution process.

Furthermore, based on the electrostatic shielding (or electrostatic protection) mechanism, the introduction of additional cations with lower reduction potentials into the electrolyte has been shown to mitigate dendritic zinc deposition during the charging process. Although these electrolyte-engineering strategies are effective in alleviating active material dissolution and interfacial instability, they still suffer from inherent limitations, such as electrolyte complexity and potential side effects on long-term electrochemical performance [16]. During repeated charge–discharge cycling, various vanadium species that are soluble in aqueous electrolytes can be generated and readily dissolved in mildly acidic media, such as $ZnSO_4$ and $Zn(CF_3SO_3)_2$ electrolytes. This dissolution process results in pronounced electrochemical performance degradation in ZIBs. On one hand, the dissolution of V_2O_5 leads to the continuous loss of electrochemically active cathode material, thereby reducing the effective energy-storage capacity. On the other hand, the dissolved vanadium species can migrate toward the zinc anode and accumulate on its surface, inducing severe anode passivation and interfacial instability.

According to previously reported studies, vanadium dissolution is governed by multiple factors, among which electrolyte pH, electrolyte composition, and applied current density are considered the most critical. Experimental observations indicate that capacity fading is more pronounced at low current densities, and this issue cannot be effectively mitigated by a single strategy alone. Consequently, a synergistic approach combining electrolyte regulation and rational electrode engineering is required to suppress vanadium dissolution and achieve enhanced cycling stability in ZIBs [5].

5.4. Formation of harmful by-products

Continuous charge–discharge cycling can induce the formation of parasitic by-products within ZIBs systems. The selection of an appropriate electrolyte is a critical parameter for achieving optimal energy-storage performance, as the occurrence of side reactions, such as the hydrogen evolution reaction (HER) and oxygen evolution reaction (OER), is highly sensitive to electrolyte pH and is ultimately governed by the electrolyte composition and salt concentration. Previous studies have demonstrated that during prolonged cycling, substantial

amounts of by-products accumulate on the cathode surface, predominantly consisting of zinc-based salts. These parasitic deposits increase interfacial resistance and accelerate capacity fading of the cathode during repeated cycling [10]. The charge–discharge processes in rechargeable batteries are intrinsically complex, and prolonged cycling significantly increases the probability of forming parasitic by-products, such as $Zn_4SO_4(OH)_6{\cdot}nH_2O$ and $Zn_3V_2O_7(OH)_2{\cdot}2H_2O$. The progressive accumulation of these by-products can induce electrode volume expansion, thereby generating mechanical stress and deteriorating the long-term cycling stability of the battery. This issue represents one of the critical challenges associated with the utilization of V_2O_5 as an active cathode material in ZIBs.

Previous studies have revealed that the primary origin of these electrochemically inert compounds is the dissolution of vanadium species from the cathode. In addition, electrolyte pH plays a decisive role in by-product formation; under conditions where the pH exceeds 2.4, vanadium species such as VO^{2+}, $VO(OH)_2^-$, and $VO_3(OH)^-$ become thermodynamically favorable and dominate in the electrolyte. Furthermore, structural and chemical changes occurring at the zinc anode can also contribute to the generation of these undesirable compounds.

Specifically, corrosion of the zinc anode releases a substantial amount of hydroxide ions into the electrolyte, thereby creating favorable conditions for the precipitation of inert by-products. This phenomenon is particularly pronounced at low current densities, where enhanced anode corrosion and aggravated vanadium dissolution increase the local reactant flux, leading to the continuous formation and accumulation of parasitic phases. The irreversible generation of such by-products inevitably results in severe degradation of the electrochemical performance of ZIBs. Accordingly, rational electrolyte selection, surface coating strategies, structural modification of V_2O_5, and effective suppression of zinc anode corrosion are regarded as viable approaches to mitigate by-product formation and improve the long-term electrochemical stability of V_2O_5-based ZIBs systems [5].

5.5. Irreversibility of layered zinc hydroxides in the presence of H^+

In a representative study, a ZIBs cell consisting of a metallic zinc anode and a $Ca_{0.34}V_2O_5{\cdot}nH_2O$ cathode was constructed to systematically investigate electrolyte pH evolution during electrochemical operation. The results indicated that during the initial stage of discharge, the electrolyte pH increased markedly due to H^+ insertion into the cathode lattice. As the discharge progressed, the pH gradually stabilized, which was attributed to the formation and accumulation of zinc-based deposits.

During the subsequent charging process, a slight decrease in pH was observed as protons were partially released from the cathode; however, the pH did not fully recover to its initial value. Further analysis revealed that these zinc-containing deposits formed with various particle sizes and were prone to remaining on the cathode surface after charging. The

interaction between these deposits and dissolved vanadium species can lead to the formation of electrochemically inactive compounds and accelerate cathode dissolution. Therefore, regulating the formation and reversibility of such deposits is critically important for enhancing the cycling stability of vanadium-based cathodes in ZIBs [4].

6. METHODS FOR MODIFYING V_2O_5 CATHODE MATERIALS IN ZINC-ION BATTERIES

Despite their high theoretical capacity and favorable layered crystal architecture, V_2O_5-based materials still suffer from several fundamental limitations that hinder their practical application as cathodes in aqueous zinc-ion batteries. These challenges mainly include vanadium dissolution in aqueous electrolytes, relatively low operating voltage and energy density, strong Coulombic interactions between Zn^{2+} ions and the host lattice, as well as insufficient structural stability during repeated charge–discharge cycling, issues that have not yet been fully resolved. To address these challenges, extensive research efforts have been devoted to improving the electrochemical performance of V_2O_5 cathodes through various structural, compositional, and surface-engineering strategies. In this section, recent modification approaches developed from multiple perspectives, including electronic conductivity enhancement, structural stabilization, and electrochemical efficiency optimization, are systematically reviewed [13].

6.1. Electrolyte modification

In aqueous ZIBs systems, the electrolyte serves as a critical component, providing continuous ionic transport pathways for Zn^{2+} ions between the zinc anode and the cathode while simultaneously defining the cell's electrochemical stability window. An ideal aqueous electrolyte should possess high ionic conductivity to ensure rapid Zn^{2+} migration and minimize polarization during charge [20]. Aqueous electrolytes offer several intrinsic advantages over their non-aqueous counterparts, including superior environmental benignity and operational safety, cost-effectiveness, and inherently high ionic conductivity. Moreover, the presence of water molecules facilitates charge-transfer processes and Zn^{2+} insertion/extraction kinetics by acting as a dielectric screening medium that buffers the high charge density of multivalent ions.

However, the electrolyte pH exerts a profound influence on the electrochemical performance of ZIBs. Both strongly acidic and alkaline conditions have been reported to induce pronounced capacity degradation and reduced Coulombic efficiency, primarily due to accelerated parasitic reactions and interfacial instability [21]. Highly alkaline electrolytes are generally unsuitable for zinc-ion batteries because they significantly accelerate zinc dendrite formation and promote the development of passivating layers on the zinc anode surface. Conversely, strongly acidic electrolytes severely deteriorate anode performance due to the intensified hydrogen evolution reaction (HER), which leads to increased parasitic reactions and

poor electrochemical reversibility [22]. To mitigate these challenges, the employment of near-neutral or mildly acidic aqueous electrolytes is generally considered a viable strategy for zinc-ion batteries. Accordingly, precise regulation of electrolyte pH and salt concentration is crucial for achieving high reversible capacity and prolonging battery lifespan. Among various near-neutral and mildly acidic electrolyte systems, zinc sulfate has been extensively adopted owing to its low cost, favorable chemical stability, and broad electrochemical stability window [7].

6.1.1. Electrolyte concentration

The Coulombic efficiency of the Zn^{2+} precipitation and dissolution process in ZIBs can be improved by adjusting the concentration of zinc-based electrolytes. The main challenge in this regard is the high hydration energy of Zn^{2+}, which hinders the reversible and rapid movement of ions. Proper control of the electrolyte concentration can effectively prevent the formation of side compounds. In these electrolytes, the increased interaction between cations and anions and the reduced interaction with water molecules provide conditions that allow for a wider stability window [23]. For example, Wang and colleagues showed that the use of a concentrated mixture of 1 mol/kg $Zn(TFSI)_2$ and 20 mol/kg LiTFSI can significantly inhibit dendrite growth and other challenges associated with zinc-ion batteries. This electrolyte suppresses the formation of $Zn(OH)_2$ in two ways: first, the high concentration of LiTFSI, and then, together with the adjustment of the pH in the near-neutral range, it reduces the hydrolysis process [24].

ZIBs employing manganese and vanadium-based cathodes are inherently plagued by cathode material dissolution, which significantly deteriorates the cycling stability of the batteries. An effective mitigation strategy to address this challenge involves the introduction of appropriate electrolyte additives into zinc-based electrolytes. In the case of manganese-based cathodes, the incorporation of $MnSO_4$ into $ZnSO_4$ electrolytes can regulate the dissolution–redeposition equilibrium of Mn^{2+} species by establishing a dynamic balance between manganese dissolution from the cathode and its reoxidation within the electrolyte, thereby enhancing the long-term cycling stability of the cathode. Moreover, the presence of $MnSO_4$ suppresses the formation of parasitic zinc sulfate by-products owing to the regulation of electrolyte pH [25]. The aluminum-based electrolyte plays a dual functional role in ZIBs systems. First, the interaction of Al^{3+} and H_3O^+ cations with the cathode material induces the formation of a hydrated layered phase, denoted as $Al_xMnO_2{\cdot}nH_2O$, which contributes to enhanced structural stability. Second, the presence of Al^{3+} effectively suppresses parasitic hydrogen evolution reaction (HER) and oxygen evolution reaction (OER), thereby expanding the electrochemical stability window of the electrolyte. Similarly, for sodium vanadate–based cathodes, the incorporation of Na_2SO_4 as an electrolyte additive has been demonstrated to significantly enhance the overall electrochemical performance of zinc-ion batteries [7,15]. This strategy operates by suppressing vanadium cathode dissolution and inhibiting zinc dendrite growth through an electrostatic protection mechanism. The presence of sodium ions, which possess a lower reduction potential than Zn^{2+} ions, effectively mitigates dendrite nucleation

and propagation. As a result, the battery delivers a high reversible specific capacity exceeding 380 mAh/g, along with a capacity retention of 82% after 1000 charge–discharge cycles [7,26].

6.2. Modification of vanadium pentoxide–based cathode materials

6.2.1. Intercalation

One of the primary contributors to capacity degradation in rechargeable batteries is the occurrence of irreversible phase transitions and the structural instability induced after repeated ion insertion. In layered cathode materials such as V_2O_5, the intrinsically limited interlayer spacing, together with high ion-diffusion energy barriers, severely hampers Zn^{2+} transport within the host lattice. This restricted ion mobility ultimately leads to sluggish reaction kinetics and accelerated capacity fading during prolonged cycling [27]. An effective strategy to address these limitations involves the pre-intercalation of guest species into the cathode lattice. Such guest species, including structural water molecules, organic moieties, anions, and cations, can stabilize the host framework, facilitate the reversible insertion/extraction of Zn^{2+}/H^+ ions, enlarge the interlayer spacing, and effectively suppress structural collapse induced by layer separation during prolonged electrochemical cycling [28]. Furthermore, the incorporation of trace amounts of metal cations or molecular species can generate additional electrochemically active sites for Zn^{2+} insertion and promote ion diffusion by effectively screening the electrostatic interactions between Zn^{2+} ions and the cathode framework. This interlayer modification strategy is widely employed to introduce foreign cations and polymeric species into vanadium oxide layers, thereby enhancing ionic transport kinetics and overall electrochemical performance [5].

In a representative study, $Co_{0.247}V_2O_5{\cdot}0.944H_2O$ was successfully synthesized via a hydrothermal route. Specifically, 0.2 M commercial V_2O_5 and 0.1 M $Co(CH_3COO)_2{\cdot}4H_2O$ were dissolved in 30 mL of a 1 M acetic acid solution, followed by hydrothermal treatment at 200 °C for 72 h. After naturally cooling to room temperature, the obtained product was thoroughly washed with ethanol and subsequently dried.

The as-synthesized $Co_{0.247}V_2O_5{\cdot}0.944H_2O$ cathode exhibits rapid and highly reversible Zn^{2+} insertion/extraction behavior at relatively high operating voltages. When assembled into a ZIBs, the system delivers an average discharge voltage of 1.7 V and a high specific capacity of 432 mAh/g at a current density of 0.1 A/g. Notably, the capacity contribution at voltages above 0.1 V reaches 227 mAh/g, accounting for approximately 52.54% of the total capacity, indicating a substantial enhancement in high-voltage energy output.

Density functional theory (DFT) calculations further reveal that, compared with pristine vanadium oxide, the interlayer incorporation of Co^{2+} ions significantly increases the Zn^{2+} adsorption energy from 1.85 eV to 2.24 eV, thereby strengthening Zn^{2+} host interactions and improving reaction kinetics. Owing to these structural advantages, the cathode demonstrates excellent rate capability, delivering a reversible capacity of 163 mAh/g even at a high current

density of 10 A/g. Moreover, outstanding cycling durability was achieved, with the battery retaining 90.26% of its initial capacity after more than 7500 charge–discharge cycles, highlighting the remarkable structural robustness of the Co-intercalated vanadium oxide framework. To elucidate the electrochemical behavior, cyclic voltammetry (CV) measurements of $Co_{0.247}V_2O_5 \cdot 0.944H_2O$ and pristine $V_2O_5 \cdot nH_2O$ cathodes were conducted using a three-electrode configuration. As illustrated in Figure 3a, electrochemical tests were performed with a stainless-steel sheet as the working electrode, metallic zinc as the counter electrode, and Ag/AgCl as the reference electrode in a concentrated aqueous electrolyte. Under identical conditions, the $Co_{0.247}V_2O_5 \cdot 0.944H_2O$ cathode exhibits two well-defined cathodic peaks at approximately 1.30 and 0.88 V versus Ag/AgCl, whereas the pristine $V_2O_5 \cdot nH_2O$ cathode shows reduction peaks at significantly lower potentials of around 0.43 and 0.16 V, indicating a pronounced upward shift in redox potentials induced by cobalt intercalation.

Figure 3b presents the galvanostatic charge–discharge profiles of $Zn\|Co_{0.247}V_2O_5 \cdot 0.944H_2O$ and $Zn\|V_2O_5 \cdot nH_2O$ cells for a comparative evaluation of electrochemical performance. The cobalt- and water-intercalated sample exhibits extended discharge plateaus in the high-voltage region and delivers a substantial capacity contribution at potentials above approximately 1.0 V. Consequently, this cathode achieves a higher average discharge voltage and enhanced gravimetric energy density. Moreover, the voltage hysteresis between the charge and discharge curves is significantly reduced for this sample, which can be ascribed to its lower internal resistance and more favorable charge-transfer kinetics as well as accelerated Zn^{2+} diffusion.

In contrast, the pristine $V_2O_5 \cdot nH_2O$ cathode predominantly operates at lower discharge voltages, resulting in a reduced average working voltage and lower specific energy. This behavior is consistent with the synergistic role of interlayer cobalt ions and structural water molecules in enlarging the interlayer spacing, reinforcing structural stability, and providing efficient diffusion pathways for Zn^{2+} ions. As illustrated in Figure 3c, upon increasing the current density from 0.1 to 10 A/g, a gradual decline in specific capacity is observed, accompanied by a slight increase in voltage polarization. Nevertheless, the discharge plateaus remain largely above 1.0 V across the entire range of current densities, ensuring the retention of a high average discharge voltage and, consequently, a relatively stable specific energy output over a wide rate window. These results indicate suppressed polarization effects and favorable Zn^{2+} insertion/extraction kinetics under high-rate conditions.

The incorporation of multivalent cations can significantly enhance the chemical and structural stability of V_2O_5 by strengthening the bonding interactions between oxygen atoms within the layered framework. In this context, Pang et al. investigated an aluminum-preintercalated V_2O_5 cathode for aqueous zinc-ion batteries. Through interlayer aluminum insertion, the crystal structure of V_2O_5 was effectively engineered to improve both structural robustness and electrochemical performance.

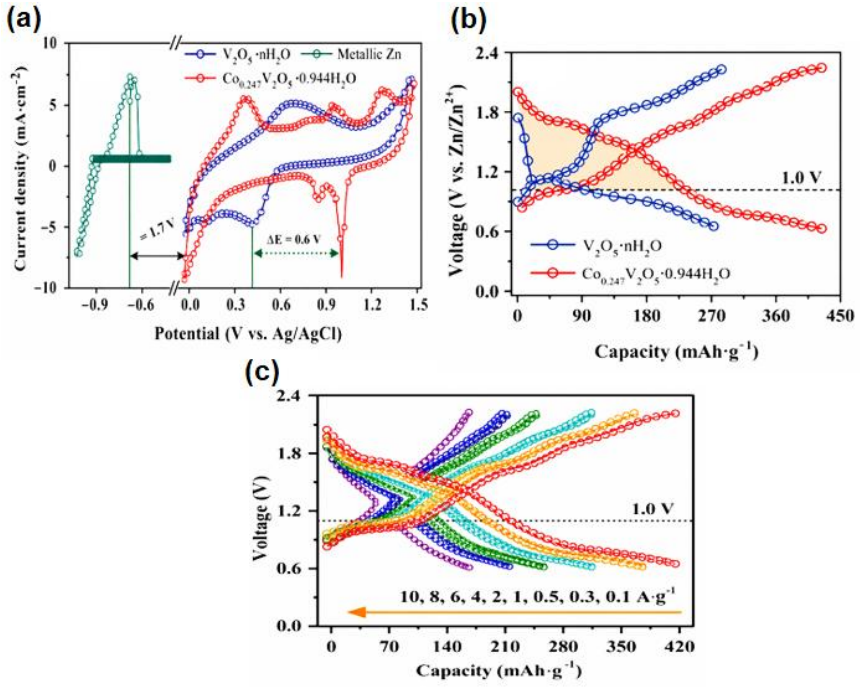

Figure 3. a: Plot of cyclic voltammetry curves of $Co_{0.247}V_2O_5 \cdot 0.944H_2O$ and V_2O_5 using a three-electrode cell with a scan rate of 1 mV/s. b: Galvanostatic charge/discharge curves of $Zn\|Co_{0.247}V_2O_5 \cdot 0.944H_2O$ $Zn\|V_2O_5$ batteries for comparison of Zn^{2+} storage. d: Galvanostatic charge and discharge curves at different current densities, reprinted with permission from [29]

In their work, Al^{3+} ions were pre-doped into the interlayer galleries of the V_2O_5 host lattice to stabilize the layered framework and facilitate Zn^{2+} storage kinetics. The $Al_{0.2}V_2O_5$ cathode was synthesized via a solution-based chemical route followed by thermal annealing at 350 °C. Electrochemical evaluations revealed that $Al_{0.2}V_2O_5$ delivers a discharge capacity of 444.8 mAh/g at a current density of 0.1 A/g, along with enhanced electronic conductivity and remarkable long-term cycling durability, retaining 61.4% of its initial capacity after 5000 cycles at 5 A/g, outperforming pristine V_2O_5.

The observed performance enhancement is primarily attributed to an increased Zn^{2+} diffusion coefficient and a reinforced crystal framework induced by aluminum pre-intercalation. These findings demonstrate that Al^{3+} incorporation represents an effective interlayer-engineering strategy for boosting the electrochemical performance and cycling stability of V_2O_5-based cathodes in aqueous ZIBs.

Figure 4a was employed to characterize the as-synthesized material and benchmark it against the pristine phase. The XRD patterns of V_2O_5 and $Al_{0.2}V_2O_5$ are presented. As expected, all diffraction peaks of pristine V_2O_5 can be well indexed to its orthorhombic crystal structure. The characteristic reflections corresponding to the (200), (001), (101), (201), and (110) planes appearing at specific diffraction angles are consistent with previously reported orthorhombic V_2O_5 phases.

For $Al_{0.2}V_2O_5$, the overall XRD profile remains largely consistent with that of pristine V_2O_5; however, the interlayer incorporation of Al^{3+} ions induces slight peak shifts and noticeable variations in diffraction intensity. These subtle structural changes confirm the successful pre-intercalation of aluminum ions into the V_2O_5 lattice, which contributes to enhanced structural stability and improved electrochemical performance.

Figure 4b depicts the galvanostatic charge–discharge profiles of the $Al_{0.2}V_2O_5$ cathode in aqueous zinc-ion batteries at various current densities. As the current density increases from 0.1 to 10 A/g, a gradual decrease in discharge capacity is observed, accompanied by shortened and steeper discharge plateaus. These features reflect kinetic limitations associated with Zn^{2+} transport and a marginal reduction in structural stability under high-rate conditions. Nevertheless, the $Al_{0.2}V_2O_5$ cathode retains robust electrochemical performance over the entire range of current densities, demonstrating excellent rate capability.

Figure 4c illustrates the long-term cycling behavior of the $Al_{0.2}V_2O_5$ cathode evaluated at a current density of 5 A/g over 5000 cycles. As shown, the discharge capacity exhibits only a minor decay during cycling and gradually stabilizes at approximately 100 mAh/g, indicating outstanding capacity retention upon prolonged cycling. Furthermore, the Coulombic efficiency progressively increases from below 40% during the initial cycles to above 80% in the intermediate stage, and ultimately approaches nearly 100% after extended cycling. These results confirm the high structural robustness and stable electrochemical reversibility of the $Al_{0.2}V_2O_5$ cathode under high-rate operating conditions.

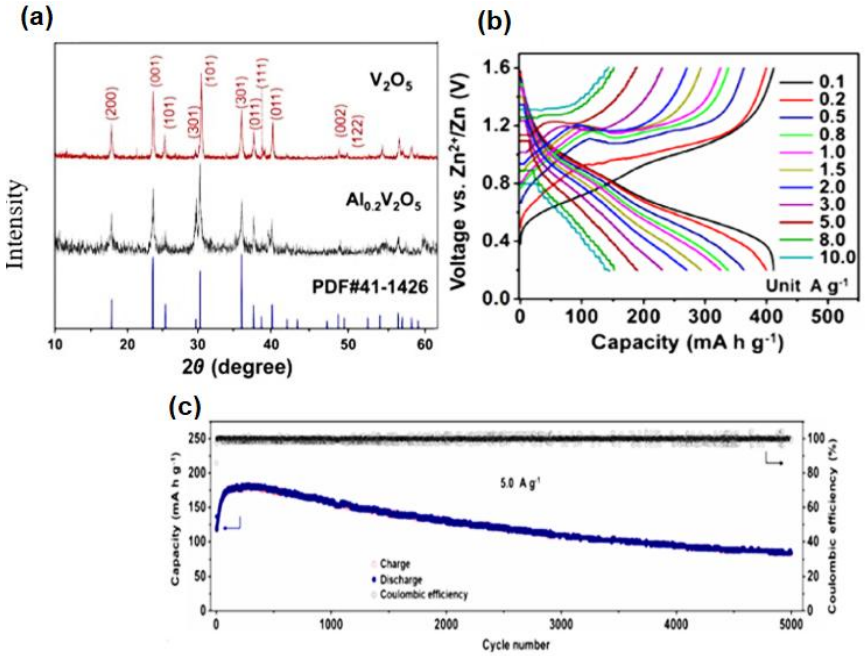

Figure 4. a: X-ray diffraction patterns of V_2O_5 and $Al_{0.2}V_2O_5$, b: Charge and discharge profiles at different current densities for $Al_{0.2}V_2O_5$, c: Long-term cycling stability of $Al_{0.2}V_2O_5$ at 5 A/g, reprint with permission from [30]

Flower-like $Cu_{0.95}V_2O_5$ nanostructures were successfully synthesized via a hydrothermal route and employed as cathode materials for aqueous zinc-ion batteries. The as-prepared electrode delivered a high initial discharge capacity of 405 mAh/g at a current density of 100 mA/g. The outstanding electrochemical performance can be primarily attributed to the Cu^{2+}/Cu^0 redox conversion process, during which the partial formation of metallic copper effectively enhances electronic conductivity and facilitates charge transfer within the electrode. Structural investigations revealed that after the initial charge–discharge cycle, the pristine $Cu_{0.95}V_2O_5$ phase undergoes an electrochemically induced phase evolution into a more open and stable $Cu_{0.4}V_2O_5$ framework, accompanied by the formation of a $Zn_3(OH)_2V_2O_7{\cdot}2H_2O$ phase. During subsequent cycling, the electrode preserves excellent structural integrity and demonstrates superior rate capability. Notably, even at a high power density of 5340 W/kg, the device maintains a considerable energy density of 88.4 Wh/kg, highlighting the potential of $Cu_{0.95}V_2O_5$ as a robust and high-performance cathode candidate for next-generation aqueous zinc-ion batteries.

As illustrated in Figure 5a, the XRD pattern of the $Cu_{0.95}V_2O_5$ sample exhibits excellent agreement with the standard JCPDS card No. 18-0463, confirming that all diffraction peaks correspond to a single-phase $Cu_{0.95}V_2O_5$ structure. This result indicates that the hydrothermal synthesis approach yields a well-crystallized material with high phase purity. Such a stable crystalline framework is highly beneficial for aqueous zinc-ion batteries, as it enables the cathode to maintain structural integrity during repeated Zn^{2+} insertion/extraction, thereby enhancing electrochemical reversibility and long-term cycling stability.

Figure 5b shows that the synthesized material possesses a flower-like hierarchical morphology composed of aggregated nanoscale building blocks, with an average particle diameter of approximately 2 μm. This hierarchical architecture provides a large specific surface area and abundant ion-accessible channels, facilitating rapid electrolyte penetration and homogeneous Zn^{2+} diffusion throughout the electrode, which collectively contribute to improved electrochemical performance.

The cyclic voltammetry curves of the $Cu_{0.95}V_2O_5$ electrode recorded at a scan rate of 1 mV/s are presented in Figure 5c. Distinct redox peaks are observed during the initial cycle, corresponding to multistep redox reactions involving the $V^{5+}/V^{4+}/V^{3+}$ and Cu^{2+}/Cu^0 couples. The good overlap and stability of these redox peaks in subsequent cycles demonstrate the high reversibility of the electrochemical processes and the robustness of the cathode structure under repeated cycling.

Figure 5d displays the galvanostatic charge–discharge profiles of the $Cu_{0.95}V_2O_5$ electrode at various current densities. Although the discharge capacity gradually decreases with increasing current density, the overall voltage profile is well preserved, indicating that the Zn^{2+} insertion/extraction mechanism remains kinetically accessible over a wide range of rates. This

behavior confirms the capability of $Cu_{0.95}V_2O_5$ to deliver appreciable capacity under high-rate conditions, making it suitable for high-power ZIBs applications.

Furthermore, the cycling performance of the $Cu_{0.95}V_2O_5$ electrode evaluated at a current density of 500 mA/g (Figure 5e) demonstrates excellent durability. The discharge capacity remains nearly constant over prolonged cycling, with negligible capacity fading, indicating high structural stability and highly reversible Zn^{2+} insertion/extraction reactions. The high-capacity retention and Coulombic efficiency approaching 100% over extended cycles further confirm the outstanding cycling durability of this cathode material, underscoring its suitability as a stable and efficient cathode for ZIBs.

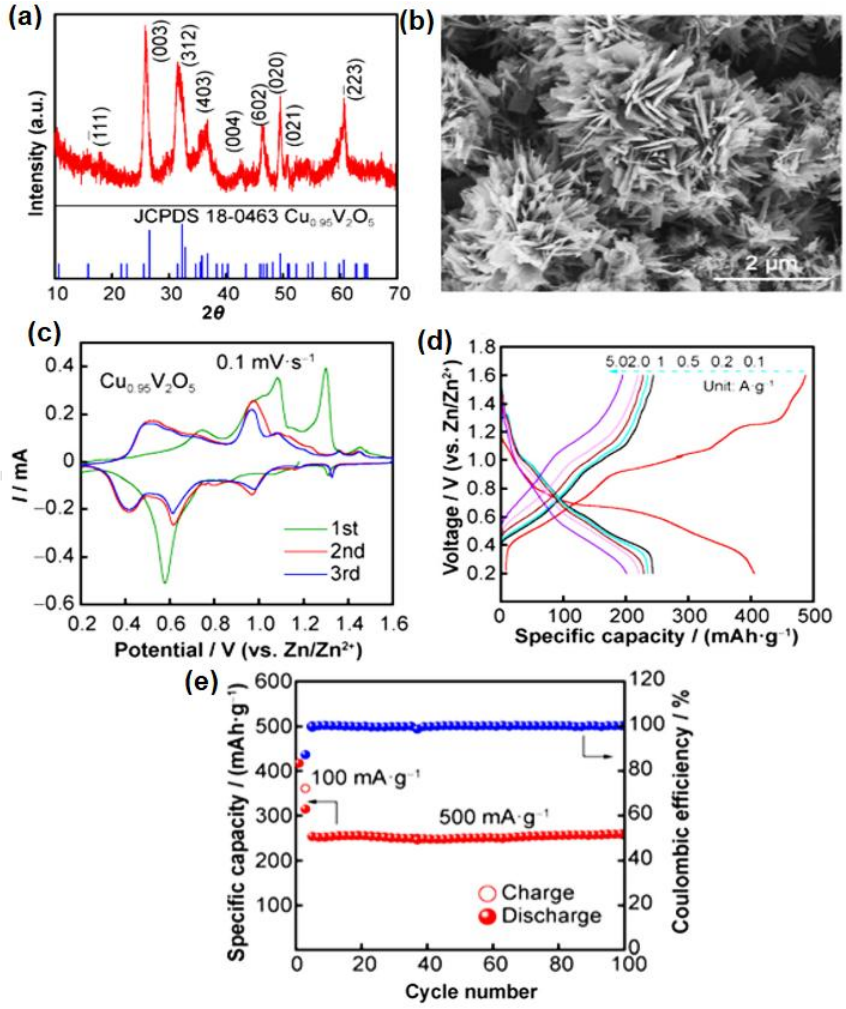

Figure 5. a: X-ray diffraction pattern of nanoscale structures with flower-like morphology, b: SEM, c: Cyclic voltammetry curves at a scan rate of 0.1 mV/s, d: Galvanostatic charge and discharge curves of $Cu_{0.95}V_2O_5$ at different current densities, e: Cyclic performance of $Cu_{0.95}V_2O_5$ nanoflorals at current densities of 500 mA/g, reprint with permission from [31]

According to the reported study, a layered vanadium-oxide-based cathode material with the chemical composition $Zn_{0.1}V_2O_5 \cdot nH_2O$ was developed for aqueous zinc-ion batteries. The

material was synthesized via a hydrothermal route using a concentrated $ZnSO_4$ solution, enabling the pre-insertion of a small amount of Zn^{2+} ions into the V_2O_5 framework. This structural design was intentionally adopted to enlarge the interlayer spacing, facilitate reversible interlayer Zn^{2+} insertion, and enhance structural stability when operating in low-cost aqueous electrolytes. Structural characterization confirms that the as-prepared material possesses a bilayer V_2O_5 xerogel architecture, in which Zn^{2+} ions and structural water molecules are accommodated within the interlayer galleries. Such a configuration leads to an expanded initial interlayer distance of approximately 10.4 Å, providing accessible diffusion pathways for Zn^{2+} ions while preserving the crystallographic integrity of the host lattice. Moreover, chemical stability tests reveal negligible vanadium dissolution in aqueous $ZnSO_4$ electrolyte, which is a critical factor contributing to the long-term electrochemical durability of the cathode. Electrochemical evaluations conducted in Zn‖ZnVO coin cells using 2 M $ZnSO_4$ electrolyte demonstrate that the cathode delivers a high specific capacity of 463 mAh/g at a current density of 0.2 A/g. Notably, even under a high current density of 10 A/g, a considerable capacity of approximately 240 mAh/g is retained, indicating favorable kinetics for interlayer Zn^{2+} transport. In terms of cycling stability, the electrode maintains about 93% capacity retention after 200 cycles at 0.2 A/g and 88% capacity retention after 20,000 cycles at 10 A/g, highlighting its exceptional long-term robustness. Mechanistic investigations suggest that the electrochemical behavior of this cathode is predominantly governed by the reversible intercalation and deintercalation of Zn^{2+} ions within the interlayer galleries of V_2O_5. The stable layered framework accommodates reversible interlayer contraction and expansion during repeated charge–discharge processes without undergoing phase transformation. Additionally, the presence of interlayer water effectively screens strong electrostatic interactions, thereby lowering diffusion barriers for Zn^{2+} ions and enabling sustained capacity at high charge–discharge rates. Overall, this study demonstrates that rational engineering of a layered V_2O_5 cathode through controlled Zn^{2+} pre-insertion and regulation of interlayer water can significantly improve interlayer Zn^{2+} storage, resulting in high specific capacity and outstanding cycling stability for aqueous zinc-ion batteries.

Figure 6a illustrates the chemical stability of the $Zn_{0.1}V_2O_5{\cdot}nH_2O$ cathode during prolonged exposure to an aqueous $ZnSO_4$ electrolyte. The material was immersed in 2 M $ZnSO_4$ for up to 30 days, and the evolution of vanadium concentration in the electrolyte as well as the corresponding pH variation was systematically monitored. As evidenced by the optical photographs, the electrolyte solution remains clear and colorless throughout the soaking period, indicating the absence of noticeable vanadium dissolution.

Quantitative analysis reveals that the vanadium concentration in the electrolyte increases slightly during the initial soaking stage and subsequently stabilizes at approximately 2 ppm, even after 30 days of immersion. This extremely low dissolution level is substantially lower than that typically observed for pristine V_2O_5 under similar conditions, suggesting that the Zn^{2+}

preinserted bilayer structure effectively suppresses vanadium leaching. Meanwhile, the pH of the $ZnSO_4$ electrolyte remains nearly constant (≈4.6) over the entire duration, further confirming that no significant parasitic dissolution reactions occur at the electrode–electrolyte interface. Overall, the results presented in Figure 6a demonstrate the exceptional chemical robustness of the ZnVO cathode in aqueous $ZnSO_4$ electrolyte, which is a crucial prerequisite for achieving long-term cycling stability in ZIBs.

Figure 6b presents a Ragone plot comparing the energy density and power density of the $Zn_{0.1}V_2O_5{\cdot}nH_2O$ cathode developed in this work with a range of previously reported cathode materials for aqueous zinc-ion batteries. As shown, the ZnVO cathode exhibits a superior balance between energy and power over a broad operating range, outperforming most reference materials in terms of energy retention, particularly at moderate and high power densities.

At relatively low power densities, the ZnVO-based system delivers a high energy density exceeding 300 Wh/kg, while maintaining a gradual decline in energy density as the power density increases. Notably, even at power densities on the order of several thousand watts per kilogram, the ZnVO cathode preserves a considerable energy output, indicating excellent rate capability and fast electrochemical kinetics.

The enhanced Ragone performance of ZnVO is attributed to its bilayer V_2O_5 architecture with enlarged interlayer spacing, which enables efficient interlayer insertion and extraction of Zn^{2+} ions. In addition, the presence of interlayer water promotes rapid ion transport and contributes to a significant pseudocapacitive component, allowing the cathode to simultaneously achieve high energy density and high power density. These results highlight the advantage of ZnVO over conventional vanadium-based and manganese-based cathodes and underscore its potential for high-performance aqueous ZIBs applications.

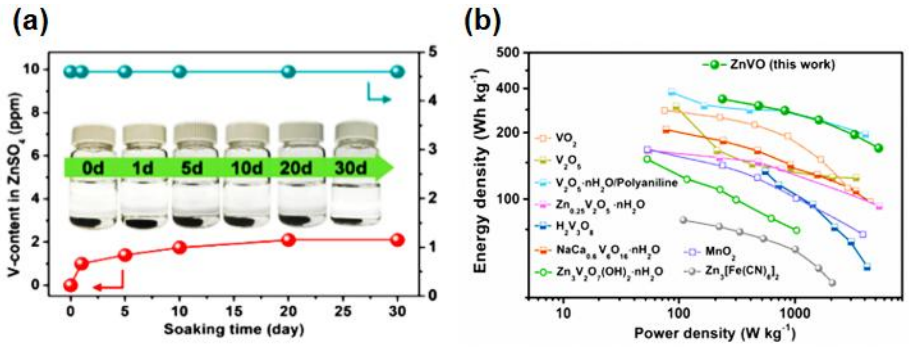

Figure 6. a: Changes in vanadium concentration and pH in 2M $ZnSO_4$ electrolyte after sample immersion, b: Energy-power performance diagram for comparing ZnVO with other reported cathodes in ZIBs, reprint with permission from [32]

To address the critical issue of vanadium dissolution in aqueous zinc-ion batteries, Liu et al. synthesized $Ba_{0.26}V_2O_5{\cdot}0.92H_2O$ (BVO-HO) nanobelts via a facile hydrothermal approach.

The co-existence of interlayer Ba^{2+} ions and structural water molecules effectively enlarges the interlayer spacing of the layered vanadate framework, thereby facilitating rapid Zn^{2+} diffusion and improving reaction kinetics. As a result, the BVO-HO cathode exhibits outstanding electrochemical performance, delivering high discharge capacities of 384.93 mAh/g at 0.05 A/g and 101.37 mAh/g at 5 A/g. Remarkably, after prolonged cycling for 2000 cycles at 5 A/g, approximately 82.7% of the initial capacity is retained, demonstrating excellent long-term cycling stability.

During repeated charge–discharge cycling, a fraction of Ba^{2+} ions gradually migrates from the cathode lattice and reacts with sulfate species in the electrolyte to form a robust in situ $BaSO_4$ interfacial layer. This self-generated protective interphase effectively suppresses vanadium dissolution and alleviates structural degradation, while remaining permeable to Zn^{2+} transport, thereby significantly extending the operational lifespan of the cathode.

As shown in Figure 7a, cycling performance evaluated at a current density of 0.5 A/g reveals that the hydrated barium vanadate cathode delivers the highest specific capacity and cycling stability among the three investigated cathodes, maintaining approximately 200 mAh/g after 50 cycles. In contrast, the anhydrous barium vanadate and pristine V_2O_5 cathodes retain capacities of only ~160 and ~110 mAh/g, respectively. Throughout the cycling process, the Coulombic efficiency remains close to 100%, indicating highly reversible Zn^{2+} insertion/extraction behavior. The superior electrochemical performance of the hydrated sample is attributed to the synergistic effect of interlayer Ba^{2+} ions and crystal water, which expand the interlayer distance, enhance ion transport, and effectively inhibit vanadium dissolution, thereby mitigating capacity fading during cycling.

Figure 7b illustrates the rate capability of the BVO-HO cathode. With increasing current density from 0.05 to 5 A/g, the specific capacity decreases stepwise; however, when the current density is reverted to lower values, the capacity is almost fully recovered. This reversible behavior reflects the high structural robustness and favorable Zn^{2+} insertion/extraction kinetics. Such performance can be ascribed to the enlarged interlayer spacing induced by Ba^{2+} ions and interlayer water, as well as the formation of a stable $BaSO_4$-type cathode–electrolyte interphase, which collectively promotes ion migration and suppresses vanadium dissolution. Consequently, the BVO-HO cathode exhibits excellent rate performance and Coulombic efficiency approaching 100%.

Figure 7c presents the galvanostatic charge–discharge profiles of the BVO-HO cathode at current densities ranging from 0.05 to 5 A/g. Distinct voltage plateaus in the range of approximately 0.6–1.3 V are observed, corresponding to stepwise redox reactions associated with Zn^{2+} insertion and extraction within the host lattice. As the current density increases, the specific capacity decreases, the voltage profiles become steeper, and the charge–discharge voltage hysteresis enlarges, which can be attributed to increased polarization, diffusion limitations, and internal resistance. Nevertheless, the preservation of the overall voltage profile

shape indicates that the dominant electrochemical reaction pathway remains unchanged, confirming the structural stability of the cathode under varying rate conditions.

Finally, the structural stability of the cathodes was further evaluated through electrolyte immersion tests, as shown in Figure 7d. For pristine V_2O_5 and anhydrous barium vanadate, the electrolyte gradually turns yellow over time, indicating the dissolution of vanadium species and interfacial instability. In contrast, the electrolyte containing the hydrated barium vanadate cathode remains nearly transparent, with no noticeable color change, confirming the effective suppression of vanadium dissolution. This enhanced stability originates from the presence of interlayer Ba^{2+} ions and structural water molecules, which reinforce the layered framework and promote the formation of a stable protective interfacial layer, ultimately leading to improved cyclability and reduced capacity degradation in ZIBs.

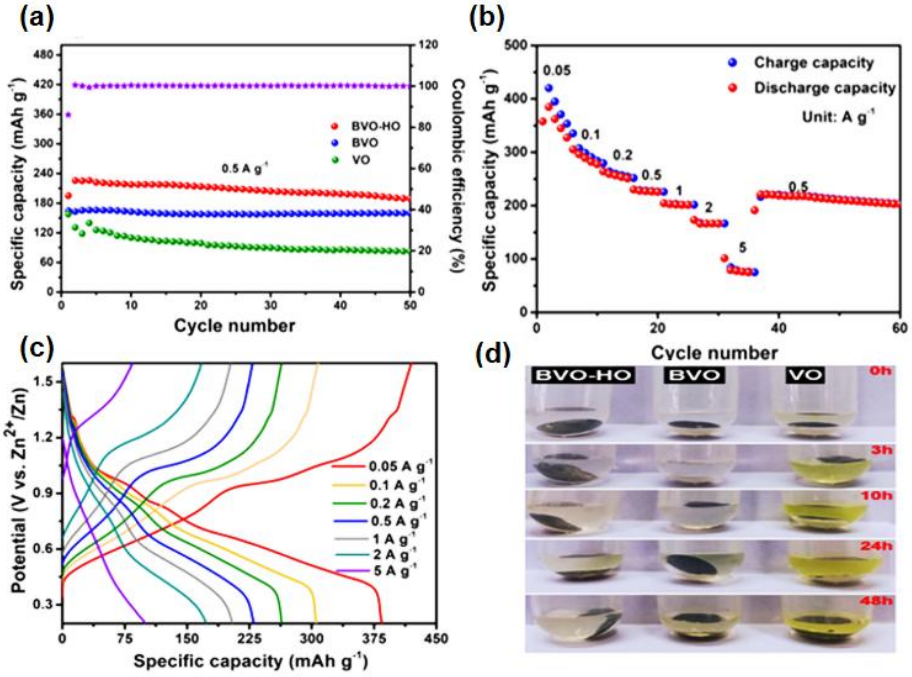

Figure 7. (a) Cycling performance of three different cathodes over 50 cycles at a current density of 0.5 A/g.(b) Rate performance of the cathode material at various current densities. (c) Galvanostatic charge–discharge profiles of the cathode at different current densities. (d) Evaluation of cathode stability in 3 M $ZnSO_4$ electrolyte at different immersion times, reprint with permission from [33]

In a related study aimed at enhancing the electrochemical performance of V_2O_5 cathodes in aqueous zinc-ion batteries, $Mn_{0.26}V_2O_5 \cdot nH_2O$ (MVOH) nanoribbons were fabricated via a combined pre-intercalation and doping strategy involving manganese ions. The coexistence of Mn^{2+}/Mn^{3+} species effectively enlarged the interlayer spacing and improved the intrinsic electronic conductivity of the host lattice, thereby constructing rapid Zn^{2+} diffusion pathways.

As a result, the MVOH cathode delivered a high specific capacity of 484 mAh/g at 0.1 A/g and 212 mAh/g at 5 A/g. Moreover, it retained approximately 95% of its initial capacity after 500 cycles at 1 A/g, with a Coulombic efficiency approaching 100%. These results demonstrate that manganese doping and pre-intercalation activate a combined insertion–quasi-capacitive storage mechanism, simultaneously enabling high capacity, long cycling stability, and enhanced conductivity in V_2O_5-based cathodes for ZIBs [34]. In another study, a Zn‖$Na_{0.33}V_2O_5$ battery configuration was designed to elucidate the role of sodium-ion intercalation in stabilizing the layered V_2O_5 framework. The inserted Na^+ ions not only expanded the interlayer spacing but also acted as structural pillars, effectively buffering repeated lattice expansion and contraction during Zn^{2+} insertion/extraction. Meanwhile, the modification of vanadium oxidation states induced by Na^+ intercalation significantly enhanced the electronic conductivity of the cathode. In this system, $Na_{0.33}V_2O_5$ nanowires were employed as the cathode material, while a 3 M $Zn(CF_3SO_3)_2$ electrolyte was used. Electrochemical evaluations revealed that the cathode delivered a high capacity of approximately 367 mAh/g at 0.1 A/g. Notably, more than 93% of the initial capacity was retained after 1000 cycles at 1 A /g, indicating excellent cycling stability and high-rate durability. These findings confirm that sodium-ion intercalation not only stabilizes the layered structure but also facilitates Zn^{2+} transport kinetics. Consequently, interlayer engineering via alkali-metal ion insertion is identified as an effective strategy to mitigate structural degradation, chemical dissolution, and low conductivity issues associated with vanadium-based cathodes in zinc-ion batteries [35].

Further corroborative evidence was provided by the pre-intercalation of potassium ions into the V_2O_5 lattice, yielding the compound $K_{0.54}V_2O_5$. The introduction of K^+ ions dramatically expanded the interlayer spacing from approximately 4.4 Å in pristine V_2O_5 to 34.9 Å, where the potassium ions functioned as stabilizing pillars and created widened ion-diffusion channels. The resulting material was synthesized in the form of nanorods with widths of several tens of nanometers and micrometer-scale lengths, and compositional analyses confirmed its stoichiometric integrity. Electrochemical testing demonstrated that the $K_{0.54}V_2O_5$ cathode delivered a capacity of 290 mAh/g at 0.2 A/g and maintained ~176 mAh/g at 5 A/g, with 97% capacity retention over 2400 cycles. The reversible capacity recovery upon lowering the current density further confirmed the high reversibility and stability of Zn^{2+} insertion/extraction processes. These results highlight that enlarged interlayer spacing and alkali-metal ion pillars are critical factors for accelerating ion transport kinetics and enhancing long-term cycling durability [36].

A comprehensive analysis of the data summarized in Table 2 indicates that structural modification strategies, such as metal-ion intercalation and the incorporation of structural water molecules into the layered V_2O_5 framework, play a crucial role in enhancing the electrochemical performance of ZIBs cathodes. These structural engineering approaches effectively enlarge the interlayer spacing, facilitate reversible Zn^{2+} insertion/extraction

processes, and significantly improve both ionic and electronic transport properties. Consequently, such modifications lead to increased specific capacity, suppressed vanadium dissolution, enhanced cycling stability, and improved Coulombic efficiency. Overall, rational engineering of the layered V_2O_5 architecture through ion and water incorporation represents an efficient and viable pathway for the development of stable, high-performance cathodes in aqueous ZIBs systems.

To provide a clearer and more systematic overview of previous investigations, all reported studies on V_2O_5–based cathodes for zinc-ion batteries have been comprehensively collected, organized, and classified in tabular form [14].

Table 2. Overview of materials inserted between layers of vanadium pentoxide

Cathodes	Electrolyte	Rate discharge capacity/mAh/g (Current Density, A/g)	Cycling capacity (retention/cycles/rates: A/g)	[Ref.]
V_2O_5	21 M LiTFSI + 1 M $Zn(CF_3SO_3)_2$	238 (0.05), 160 (5)	90%/2000/2	[37]
V_2O_5	3 M $Zn(CF_3SO_3)_2$	460 (0.5), 386 (10)	91.1%/400/5	[38]
$Na_{0.33}V_2O_5$	0.2 M $Zn(CF_3SO_3)_2$	395 (0.1), 91 (20)	75%/3000/5	[35]
$Na_{0.56}V_2O_5$	3 M $ZnSO_4$ + 0.5 M Na_2SO_4	295 (0.1), 91 (2)	87%/1000/1	[39]
$K_{0.5}V_2O_5$	3 M $ZnSO_4$	436.2 (0.5), 177.1 (3)	75%/3000/5	[40]
$K_{0.54}V_2O_5$	3 M $Zn(CF_3SO_3)_2$	244 (0.2), 190 (5)	97%/2400/5	[36]
$K_{0.23}V_2O_5$	2 M $Zn(CF_3SO_3)_2$	284 (0.1), 118 (2)	92.8%/500/2	[41]
$Cu_{0.95}V_2O_5$	3 M $Zn(CH_3F_3SO_3)_2$	318 (0.1), 195 (5)	92%/1000/5	[42]
$Na_{0.58}V_2O_5{\cdot}0.11\ H_2O$	2 M $Zn(CF_3SO_3)_2$	540 (0.2), 132 (10)	91.2%/100/1	[43]
$Zn_xV_2O_5{\cdot}nH_2O$	3 M $Zn(CF_3SO_3)_2$	434.6 (0.5), 227.8 (10)	218 mAh/g/1000/2	[44]
$Zn_{0.3}V_2O_5{\cdot}1.5\ H_2O$	3 M $Zn(CF_3SO_3)_2$	426.3 (0.2), 265.2 (10)	96%/20000/10	[45]
$Zn_{0.1}V_2O_5{\cdot}nH_2O$	2 M $ZnSO_4$	463 (0.2), 240 (10)	88%/20000/10	[32]
$Mg_{0.2}V_2O_5{\cdot}0.8\ H_2O$	3 M $Zn(CF_3SO_3)_2$	344 (0.1), 218 (10)	83.7%/10000/5	[46]
$Mg_{0.19}V_2O_5{\cdot}0.99\ H_2O$	3 M $Zn(CF_3SO_3)_2$	425.6 (0.2), 210.4 (5)	98.1%/5000/5	[47]
$Ca_{0.04}V_2O_5{\cdot}1.74\ H_2O$	3 M $Zn(CF_3SO_3)_2$	400 (0.05), 187 (10)	100%/3000/10	[48]
$Ba_{0.26}V_2O_5{\cdot}0.92\ H_2O$	3 M $ZnSO_4$	384.93 (0.05), 101.37 (5)	82.7%/2000/5	[33]
$Ba_{0.23}V_2O_5{\cdot}1.1\ H_2O$	3 M $Zn(CF_3SO_3)_2$	378 (0.1), 172 (5)	93%/2000/5	[49]
$Mn_{0.26}V_2O_5{\cdot}nH_2O$	3 M $ZnSO_4$	484 (0.1), 212 (5)	95%/500/1	[50]
$Co_{0.247}V_2O_5{\cdot}0.944\ H_2O$	21 M LiTFSI + 1 M $Zn(CF_3SO_3)_2$	432 (0.1), 163 (10)	90.26%/7500/4	[29]
$Ni_{0.22}V_2O_5{\cdot}0.94\ H_2O$	3 M $Zn(CF_3SO_3)_2$	442 (0.1), 180 (15)	87.5%/1500/10	[51]
$Cu_{0.18}V_2O_5{\cdot}0.72\ H_2O$@CC	3 M $Zn(CF_3SO_3)_2$	217.8 (0.1), 106.1 (5)	~120 mAh/g/2000/1	[52]
$K_{0.09}Mg_{0.03}V_2O_5{\cdot}nH_2O$	3 M $Zn(CF_3SO_3)_2$	423 (0.1), 210 (2)	72%/2000/4	[53]
$Zn_{0.25}(NH_4)V_2O_5{\cdot}H_2O$	2 M $Zn(CF_3SO_3)_2$	367 (0.1), 93 (1.5)	84.6%/1220/1	[54]

6.2.2. Coating

To effectively suppress vanadium dissolution in vanadium-based cathodes, a conformal carbon layer was uniformly deposited onto V_2O_3 nanorods via a polydopamine-assisted coating strategy. The resulting carbon shell markedly enhances the electronic conductivity and structural robustness of the nanorods compared with pristine V_2O_3. Benefiting from this surface

engineering, the V_2O_3@C nanorods exhibit significantly improved electrochemical performance. Notably, a high reversible capacity of 290 mAh/g is delivered at a current density of 1 A/g, which is substantially higher than that of the bare V_2O_3 counterpart. These results underscore the critical role of carbon-based surface coatings in improving charge-transfer kinetics, structural stability, and overall electrochemical performance of zinc-ion batteries [4]. In a related study, a conductive polypyrrole polymer layer was coated onto the surface of V_2O_5 to enhance electronic conductivity and mitigate vanadium dissolution during electrochemical cycling. This polymeric coating effectively improves cycling durability and rate capability. As a result, the V_2O_5@PPy electrode delivers an initial discharge capacity of 109.6 mAh/g and retains approximately 95.6% of its initial capacity after 300 cycles, whereas pristine V_2O_5 preserves only 35.9% of its capacity under identical conditions. Furthermore, even at a high current density of 5 A/g, the V_2O_5@PPy cathode maintains a specific capacity of 68.4 mAh/g, highlighting the effectiveness of conductive polymer coatings in stabilizing vanadium-based cathodes for aqueous ZIBs [55]. In another study aimed at mitigating the issues of low intrinsic electronic conductivity and structural dissolution of vanadium-based cathodes in aqueous zinc-ion batteries, a V_2O_5@PEDOT composite was fabricated by conformally coating the conductive polymer poly onto the surface of V_2O_5 nanosheets. This surface-engineering strategy effectively enhances charge-transport properties and stabilizes the cathode framework.

Electrochemical characterization demonstrated that the PEDOT coating substantially improves both the reversible capacity and long-term cycling stability of the cathode. Specifically, the V_2O_5@PEDOT electrode delivers a high specific capacity of 390 mAh/g at a current density of 0.3 A/g and maintains a capacity of 101 mAh/g even at an ultrahigh current density of 20 A/g, indicating excellent rate capability. Moreover, after more than 1000 charge–discharge cycles at 5 A/g, the electrode preserves outstanding cycling durability with a Coulombic efficiency approaching 100%, underscoring the effectiveness of conductive polymer coatings in stabilizing vanadium-based cathodes for high-performance zinc-ion batteries [56].

6.2.3. Doping

According to the results reported by Li et al, cobalt incorporation into the V_2O_5 lattice via a combined hydrothermal synthesis and subsequent calcination treatment markedly enhances the electrochemical performance of V_2O_5 as a cathode material for ZIBs. Electrochemical measurements revealed that an optimized cobalt doping level of 0.075 mmol enables the cathode to deliver a high specific capacity of 437 mAh/g at a current density of 0.2 A/g, while maintaining a remarkable capacity of 359 mAh/g even at a high current density of 5 A/g.

Moreover, the hollow architecture induced by cobalt doping effectively facilitates electrolyte penetration and ion transport, while simultaneously accommodating volume variation of the electrode during repeated charge–discharge cycling. This structural design significantly enhances the mechanical integrity of the cathode and contributes to prolonged

cycling lifespan. In addition, cobalt incorporation strengthens the V–O bonding framework and suppresses vanadium dissolution during electrochemical cycling, thereby improving electrochemical stability and overall performance. Collectively, these results demonstrate that cobalt doping effectively enhances electronic conductivity, increases reversible capacity, reinforces structural stability, and extends the operational lifetime of V_2O_5-based cathodes. Consequently, cobalt doping represents a promising and effective strategy for advancing high-performance cathode materials in ZIBs battery systems [57]. In another study, an aluminum-ion doping strategy was employed to mitigate the intrinsic limitations of V_2O_5, including its low electronic conductivity and sluggish Zn^{2+} diffusion kinetics. In this approach, V_2O_5 was rapidly quenched into an $Al_2(SO_4)_3$ solution following high-temperature calcination, enabling the incorporation of Al^{3+} ions into the V_2O_5 crystal lattice while simultaneously generating a high concentration of oxygen vacancies. Electrochemical evaluations revealed that the Al-doped V_2O_5 cathode delivers an ultrahigh specific capacity of 532 mAh/g at a current density of 0.1 A/g and retains approximately 76% of its initial capacity after prolonged cycling for 5000 cycles at 5 A/g, demonstrating exceptional cycling durability. Furthermore, electrochemical impedance spectroscopy results indicated a substantial reduction in charge-transfer resistance and a pronounced enhancement in electronic conductivity. Density functional theory (DFT) calculations further confirmed that Al^{3+} incorporation significantly lowers the Zn^{2+} diffusion energy barrier from 0.36 eV to 0.09 eV, thereby facilitating reversible Zn^{2+} insertion and extraction processes. Overall, this study demonstrates that aluminum-ion doping, coupled with defect engineering, represents an effective strategy for simultaneously enhancing capacity, cycling stability, and electronic conductivity of V_2O_5-based cathodes in ZIBs [58].

Guo et al. employed a tin-ion doping strategy to address the intrinsic limitations of V_2O_5 cathodes in aqueous zinc-ion batteries. In their approach, V_2O_5 and $SnCl_5{\cdot}5H_2O$ precursors were subjected to a hydrothermal process, followed by drying, to obtain a Sn-doped $V_2O_5{\cdot}nH_2O$ compound. This synthesis route enables the incorporation of Sn ions into the V_2O_5 lattice during crystal growth, resulting in homogeneous lattice substitution. In addition to modulating the V^{5+}/V^{4+} redox ratio, tin incorporation induces the formation of oxygen vacancies within the crystal framework. These defect sites effectively enhance electronic conductivity and create additional diffusion pathways for Zn^{2+} ions.

Electrochemical evaluations demonstrated that the Sn-doped $V_2O_5{\cdot}nH_2O$ cathode delivers a high discharge capacity of 374 mAh/g at a current density of 0.1 A/g and maintains a remarkable capacity of 301 mAh/g even at an ultrahigh rate of 10 A/g. Moreover, the cathode retains approximately 87.5% of its initial capacity after 2000 cycles at 2 A/g, indicating excellent long-term cycling stability. Compared with pristine aqueous V_2O_5, the Sn-doped sample exhibits substantially improved capacity, rate capability, and cycling durability. Overall, this study demonstrates that tin-ion doping via a hydrothermal route represents a facile

and effective strategy to enhance electronic conductivity, boost specific capacity, stabilize the crystal structure, and suppress vanadium dissolution, thereby enabling durable and high-performance vanadium-based cathodes for ZIBs [59].

In another study, a cerium-ion doping strategy was employed to alleviate the intrinsic limitations of V_2O_5 cathodes, such as low electronic conductivity and inadequate structural stability, in aqueous zinc-ion batteries. In this approach, Ce^{3+} ions partially substitute V^{5+} ions within the vanadium pentoxide crystal lattice, resulting in an expansion of the lattice parameters due to the larger ionic radius of Ce^{3+}. XRD analysis reveals a systematic shift of diffraction peaks toward lower angles, while X-ray photoelectron spectroscopy (XPS) confirms a variation in the V^{4+}/V^{5+} ratio, indicating that cerium incorporation is accompanied by the generation of abundant oxygen vacancies. These defect-induced structural modifications effectively enhance electronic conductivity, improve structural robustness during repeated charge–discharge cycling, and provide more accessible diffusion pathways for Zn^{2+} ions. Electrochemical evaluations demonstrate that the Ce^{3+}-doped V_2O_5 cathode delivers a higher specific capacity compared to pristine V_2O_5, along with significantly enhanced cycling stability. Moreover, under high current densities, the doped cathode maintains favorable rate capability, which can be attributed to the increased ion-transport channels and improved structural flexibility induced by cerium doping. Overall, this study demonstrates that Ce^{3+} ion doping represents an effective lattice-engineering strategy to enhance specific capacity, improve Coulombic efficiency, and reinforce long-term cycling stability of V_2O_5–based cathodes for ZIBs [60].

7. CONCLUSION

Zinc-ion batteries have emerged as promising candidates for large-scale grid energy storage applications owing to their high theoretical specific capacity, favorable electrochemical redox potentials, intrinsic safety characteristics, and the abundant availability and low cost of zinc-based resources. Nevertheless, the practical advancement of this technology is primarily hindered by the limited availability of cathode materials that simultaneously deliver high reversible capacity and long-term cycling stability, which are critical for the durability and efficiency of ZIBs in large-scale applications [7,10,61]. In recent years, extensive research efforts have been devoted to Zn/V_2O_5-based battery systems. If an optimal synergy between structurally engineered V_2O_5 cathodes, zinc metal anodes, and advanced electrolyte formulations can be realized, this system holds significant promise for large-scale energy storage applications. This review provides a comprehensive overview of the crystal structure, physicochemical properties, and electrochemical characteristics of V_2O_5 materials, followed by a detailed discussion of Zn^{2+} storage mechanisms in various vanadium oxide cathodes. To date, four dominant energy storage mechanisms have been identified, including reversible Zn^{2+} intercalation/deintercalation, co-intercalation of H^+ and Zn^{2+} ions, proton-only

insertion/extraction, and a combined displacement–intercalation mechanism. Subsequently, commonly employed synthesis routes for V_2O_5-based materials, such as hydrothermal, sol–gel, thermal decomposition, casting, and related methods, are systematically analyzed with emphasis on their respective advantages and inherent limitations. In addition, various modification strategies aimed at enhancing the electrochemical performance of V_2O_5 cathodes are critically reviewed, including guest-species pre-intercalation, composite engineering, defect modulation, and morphology control. Among these approaches, ion pre-intercalation is recognized as an effective strategy to stabilize the layered framework and facilitate ion transport, wherein diverse guest species, such as metal cations and neutral molecules, can be introduced into the V_2O_5 host lattice to tailor its electrochemical behavior. Moreover, hybridization of V_2O_5 with conductive components plays a crucial role in improving electronic conductivity and boosting specific capacity, while defect engineering and rational nanostructure design can increase electrochemically active sites and mitigate mechanical stress associated with repeated ion insertion/extraction processes. Despite these advances, several critical challenges still impede the practical commercialization of Zn/V_2O_5 battery systems, including the dissolution of electrochemically active vanadium species, formation of irreversible and parasitic by-products, incomplete understanding of ion storage mechanisms, relatively low energy and power density, and sluggish charge-transfer kinetics. Addressing these issues is essential for unlocking the full potential of V_2O_5-based cathodes in next-generation aqueous zinc-ion batteries [13]. With the continuous advancement of cutting-edge analytical techniques and the adoption of emerging experimental methodologies, ZIBs systems exhibit considerable prospects for scalable integration and are increasingly regarded as economically viable and environmentally sustainable alternatives to traditional lithium-ion energy storage systems in the near term [3].

Declarations of interest

The authors declare no conflict of interest in this reported work.

REFERENCES

[1] P.A. Owusu, and S.A. Sarkodie, Cogent Engin. 3 (2016) 1167990.

[2] K. Lolupmani, J. Cao, D. Zhang, C. Yang, X. Zhang, and J. Qin, Journal of Metals, Materials and Minerals 34 (2024) 2084.

[3] W. Zheng, Z. Sun, Zhen. Gu, X. Wu, and L. Niu, Adv. Mater. Technol. (2025) 2500320.

[4] K. Zhu and W. Yang, Acc. Chem. Res. 57 (2024) 2887.

[5] A. Guo, Z. Wang, L. Chen, W. Liu, K. Zhang, L. Cao, B. Liang, and D. Luo, ACS Nano 18 (2024) 27261.

[6] T. Zhou, L. Zhu, L. Xie, Q. Han, X. Yang, L. Chen, G. Wang, and X. Cao, J. Colloid Interface Sci. 605 (2022) 828.

[7] S. Mallick, and R. Raj, Chem. Sus. Chem. 14 (2021) 1987.
[8] T. Juran, J. Young, and M. Smeu, ACS Paragon Plus Environment 122 (2018) 8788.
[9] L. Chen, Q. An, and L. Mai, Adv. Mater. Interfaces 6 (2019) 1900387.
[10] G. Li, L. Sun, Sh. Zhang, Ch. Zhang, H. Jin, K. Davey, G. Liang, S. Liu, J. Mao, and Z. Guo, Adv. Funct. Mater 34 (2024) 2301291.
[11] Ch. Xu, H. Du, B. Li, F. Kang, and Y. Zeng, Electrochem. Solid-State Lett. 12 (2009) A61.
[12] S. Saadi-motaallegh, M. Javanbakht, H. Omidvar, and S. Habibzadeh, Journal of Alloys and Compounds 963 (2023) 171119.
[13] T. Zhou, and G. Gao, Nano Energy 127 (2024) 109691.
[14] Y. Wang, H. Chen, Sh. Zhang, L. Hou, X. Li and C. Yuan, Next Energy 4 (2024) 100119.28.
[15] N. Zhang, Y. Dong, M. Jia, X. Bian, Y. Wang, M. Qiu, J. Xu, Y. Liu, L. Jiao, and F. Cheng, ACS Energy Lett. 3 (2018) 1366.
[16] F. Wan, L. Zhang, X. Dai, X. Wang, Z. Niu, and J. Chen, Nature Commun. 9 (2018) 1656.
[17] K. Zhu, T. Wu, S. Sun, W. van, M. Stefik, and K. Huang, Energy Storage Materials 29 (2020) 60.
[18] W. Sun, F. Wang, S. Hou, C. Yang, X. Fan, Z. Ma, T. Gao, F. Han, R. Hu, M. Zhu, and C. Wang, J. Am. Chem. Soc. 139 (2017) 9775.
[19] T. Zhou, Q. Han, L. Xie, X. Yang, L. Zhu, and X. Cao, Chem. Rec. 22 (2022) e202100275.
[20] W. Kao, R. Pornprasertsuk, P. Thamyongkit, T. Maiyalagan, and S. Kheawhom, J. Electrochem. Soc. 166 (2019) A1063.
[21] J. Shin, J. Lee, Y. Park, and J.W. Choi, Chem. Sci. 11 (2020) 2028.
[22] J. Parker, C. Chervin, I. Pala, M. Machler, M. Burz, J. Long, and D. Rolison, Science 356 (2017) 415.
[23] V. Azov, K. Egorova, M. Seitkalieva, A. Kashina, and V. Ananikov, Chem. Soc. Rev. 47 (2018) 1250.
[24] F. Wang, O. Borodin, T. Gao, X. Fan, W. Sun, F. Han, A. Faraone, J. Dura, K. Xu, and C. Wang, Nature Materials 17 (2018) 543.
[25] S. Heum Kim, and S. Mo Oh, Journal of Power Sources 72 (1998) 150.
[26] R. Trócoli, G. Kasiri, and F. La Mantia, Journal of Power Sources 400 (2018) 167.
[27] B. Tang, L. Shan, S. Liang, and J. Zhou Energy Environ. Sci. 12 (2019) 3288.
[28] Y. Kim, Y. Park, M. Kim, J. Lee, K. Kim, and J. Choi, Nature Commun. 13 (2022) 237.
[29] L. Ma, L. Na, C. Long, B. Dong, F. Daliang, Z. Liu, Y. Zhao, X. Li, J. Fan, S. Chen, S. Zhang, and C. Zhi, Advanced Functional Materials 29 (2019) 1906142.

[30] Q. Panga, W. He, X. Yu, S.Yang, H. Zhaob, Y. Fu, M. Xing, Y. Tiana, X. Luoa, and Y. Wei, Applied Surface Science 538 (2021) 148043.
[31] X. Yu, F. Hu, Zh. Guo, L. Liu, G. Song, and K. Zhu, Rare Met. 41 (2022) 29.
[32] K. Zhu, T. Wu, W. Bergh, M. Stefik, and K. Huang, ACS Nano 15 (2021) 10678.
[33] S. Luo, X. Cao, Q. Su, Y. Zhang, S. Liu, X. Xie, S. Liang, and A. Pan, ACS Appl. Energy Mater. 4 (2021) 6197.
[34] Y. Jiang, H. Xu, L. Ren, M. Ji, X. Shen, and S. Li, Energy Fuels 35 (2021) 17948.
[35] P. He, G. Zhang, X. Liao, M.Yan, X. Xu, Q. An, J. Liu, and L. Mai, Adv. Energy Mater. 8 (2018) 1702463.
[36] P. Wu, T. Xu, Y. Chen, Q. Yang, J. Wang, Y. Liu, and Y. Li, ACS Appl. Energy Mater. 5 (2022) 1656.
[37] P. Hu, M. Yan, T. Zhu, X. Wang, X. Wei, J. Li, L. Zhou, Z. Li, L. Chen, and L. Mai, ACS Appl. Mater. Interfaces 9 (2017) 42717.
[38] N. Zhang, Y. Dong, M. Jia, X. Bian, Y. Wang, M. Qiu, J. Xu, Y. Liu, L. Jiao, and F. Cheng, ACS Energy Lett. 3 (2018) 1366.
[39] P. Gao, Q. Ru, H. Yan, Sh. Cheng, Y. Liu, X. Hou, Li. Wei, and F. Ling, Chem Electrochem. 7 (2020) 283.
[40] Y. Hao, Sh. Zhang, P. Tao, T. Shen, Z. Huang, J. Yan, and Y. Chen, ChemNanoMat 6 (2020) 797.
[41] W. Zhang, C. Tang, B. Lan, L. Chen, W. Tang, C. Zuo, S. Dong, Q. An, and P. Luo, Journal of Alloys and Compounds, 819 (2020) 152971.
[42] X. Yu, F. Hu, Z. Guo, L. Liu, G. Song, and K. Zhu, Rare Met. 41 (2021) 29.
[43] D. Pan, T. Liu, Y. Zhang, H. Liu, M. Ding, and L. Chen, Journal of the Taiwan Institute of Chemical Engineers, 127 (2021) 276.
[44] K. Hu, D. Jin, Y. Zhang, L. Ke, H. Shang, Y. Yan, H. Lin, K. Rui, and J. Zhu, Journal of Energy Chemistry 61 (2021) 594.
[45] L. Wang, K. Huang, J. Chen, and J. Zheng, Sci. Adv. 5 (2019) eaax4279.
[46] J. Guan, L. Shao, L. Yu, Sh. Wang, X. Shi, J. Cai, and Z. Sun, Chem. Eng. 443 (2022) 136502.
[47] W. Zhou, J. Chen, M. Chen, A. Wang, A. Huang, X. Xu, J. Xu, and C. Wong, J. Mater. Chem. A 8 (2012) 8397.
[48] M. Du, F. Zhang, X. Zhang, W. Dong, Y. Sang, J. Wang, H. Liu, and S. Wang, Sci. China Chem. 63 (2020) 1767.
[49] X. Qin, Y. Du, P. Zhang, X. Wang, Q. Lu, A. Yang, and J. Sun, Miner Metall. Mater. 28 (2021) 1684.
[50] Y. Jiang, H. Xu, L. Ren, M. Ji, X. Shen, and S. Li, Energy Fuels 35 (2021) 17948.
[51] Y. Liu, J. Lv, T. Cao, Y. Gong, and D. Zhang, Chem. Engi. J. 441 (2022) 136007.
[52] J. Ren, P. Hong, Y. Ran, Y. Chen, X. Xiao, and Y. Wang, Chem. Front. 9 (2022) 792.

[53] Z. Feng, Y. Zhang, J. Sun, Y. Liu, H. Jiang, M. Cui, T. Hu, and C. Meng, Chem. Engin. J. 433 (2022) 133795

[54] J. Wu, Z. Yang, H. Chen, L. Deng, Y. Rong, and Z. Fu, Applied Surface Sci. 592 (2022) 153137

[55] R. Dong, T. Zhang, J. Liu, H. Li, D. Hu, X. Liu, and Q. Xu, Chem. Electrochem. 9 (2022) 202101441.

[56] S. Volkov, N. Eliseeva, A. Kamenskii, I. Volkov, G. Tolstopjatova, V. Glumov, L. Fu, and V. Kondratiev, Nanomaterials 12 (2022) 3896.

[57] Q. Li, N. Yu, L. Li, B. Sun, X. Chen, F. Wei, Q. Wang, Y. Sui, J. He, Z. Zhang, Journal of Power Sources, 628 (2025) 235895.

[58] H. Jiang, W. Gong, Y. Zhang, X. Liu, M. Waqar, J. Sun, Y. Liu, X. Dong, Ch. Meng, and Z. Pan, J. Wang, J. Energy Chem. 70 (2022) 52

[59] K. Guo, W. Cheng, H. Liu, W She, Y. Wan, H. Wang, H. Li, Z. Li, X. Zhong, J. Ouyang, and N. Yu, Crystals 12 (2022) 1617.

[60] C. Ganesh, B. Krushna, I. Pruthviraj, G. Ramakrishna, S. Sharma, A. George, S. Mishra, U. Premkumar, K. Manjunatha, Sh. Wu, H. Chih Kuo, V. Shivakumar, S. Devaraja, and H. Nagabhushana, Journal of the Taiwan Institute of Chemical Engineers 174 (2025) 106223.

[61] S. Saadi-motaallegh, M. Javanbakht, H. Omidvar, and S. Habibzadeh, Journal of Alloys and Compounds 914 (2022) 165249.